NRC RAI Letter No. PTN-RAI-LTR-047

SRP Section: 02.04.06 – Probable Maximum Tsunami Flooding

Question from Hydrological and Meteorology Branch (RHMB)

NRC RAI Number: 02.04.06-8 (eRAI 6225)

To meet the requirements of GDC 2, 10 CFR 52.17, and 10 CFR Part 100, FPL should provide an assessment of the Probable Maximum Tsunami (PMT) for the proposed site. Section C.I.2.4.6.3 of Regulatory Guide 1.206 (RG 1.206) provides specific guidance with respect to the source characteristics needed to determine the PMT. Provide justification that source parameters for the Cape Fear landslide from Hornbach et al. (2007) are conservative, with regard to not only the upper part of the landslide, but also the downslope region of failure. If the source parameters for this potential PMT source are revised, discuss how the revised source affects PMT water levels at the site.

FPL RESPONSE:

A new FSAR Subsection 2.4.6.4.2 (see Associated COLA Revisions) evaluates the impact at the Turkey Point Units 6 & 7 site from a tsunami generated as a result of a hypothetical submarine landslide event at a site identified as the Cape Fear Slide. It concludes, based on modeling results and assessments inferred from recent published literature on the subject, that the flood risk at the Units 6 & 7 site from the Cape Fear Slide will be bounded by the postulated PMT, i.e., the 1755 Lisbon Earthquake tsunami, as described in Subsection 2.4.6.4.1.

In response to RAI 02.04.06-8, additional discussion on the source characteristics of the Cape Fear Slide including the downslope region of the failure is provided. Further, a quantitative assessment of the tsunami generation at the Cape Fear Slide using a set of conservative source parameters, and its propagation towards the Units 6 & 7 site using the numerical models, NHWAVE (Version 1.1) and FUNWAVE (Version 1.1), developed and maintained by the University of Delaware, is described.

Specifically, the response explains how the postulated Cape Fear Slide was represented in the model and describes the estimation of the wave shape and size generated by this slide, The numerical simulations of the tsunami wave propagation and coastal inundation at the Units 6 & 7 site based on two alternative assumptions for the initial wave, corresponding to a dynamic source and a static source generated by the Cape Fear Slide, is also presented.

As demonstrated in the following sections, the additional information provided on the source characterization of the Cape Fear Slide, in conjunction with the numerical tsunami generation and propagation model simulations performed, support the conclusion given in FSAR Section 2.4.6.5 that the maximum water level at Turkey Point Units 6 & 7 caused by a tsunami from the Cape Fear Slide would be lower than the maximum water level predicted for the PMT.

The Cape Fear Slide

The Cape Fear Slide occurred on the Atlantic continental slope and rise approximately 200 kilometers southeast of Cape Fear, North Carolina. The Cape Fear Slide headwall is described as an amphitheater-shaped scarp centered on a lower slope at a depth of approximately 2300 to 2600 meters, 50 kilometers long, and approximately 120 meters high. Within the headwall's failure area, two large salt diapirs project above the sea floor. A complex of slumps extends more than 40 kilometers upslope from the major headwall scarp, and mass-movement deposits are traceable for more than 400 kilometers downslope to a water depth of over 5.4 kilometers on the Hatteras Abyssal Plain (References 1, 2, 3, 4 and 5). Longitudinal lines in the 1987 GLORIA side-scan sonar image, Figure 1, (reproduced from Figure 4 in Reference 1), are interpreted as evidence of mass movement. The longitudinal lines represent both debris chutes between the salt diapirs at the head of the landslide area indicated by the Label A in Figure 1, and debris flow paths further downslope indicated by the Label B (Reference 1). In the proximal area of the landslide, Label C in Figure 1, an area of irregular, hummocky topography on the sea floor provides evidence of mass movement. At the distal portion of the slide, the landslide material extends across an older slope failure, the Cape Lookout Slide (Reference 1).

Multibeam swath bathymetric data from the SeaBeam 2100/12 system and single channel Chirp data using a Knudsen 320B/R echosounder acquired in 2007 (Reference 5), provide the basis for a new interpretation of the Cape Fear slide. The data revealed at least five major escarpments (labeled S1 through S5 in Figure 2 of Reference 5). The S1 scarp is the westward and shallowest of the scarps, at approximately 890 meters below sea level, and with a crown-shaped headwall that extends 40 kilometers downslope of both sides of the slide scar. The S1 scarp crosscuts the S4 and S5 scarps and extends upslope of the main headwall (S4 and S5 headwalls). The S2 and S3 scarps are located within the S1 debris field. The S2 scarp is approximately 20 kilometers long and approximately three kilometers wide chute that abruptly widens downslope. The approximate headwall height for the S2 scarp is at least 30 meters. The S3 scarp is associated with the smallest disrupted area and has a height of at least 20 meters above the rupture surface. The main headwall scarp, S4, is likely the largest slide in the complex with an approximately 120-meter high headwall that extends over approximately 50 kilometers. The S5 scarp intersects the northern flank of the S4 scarp and is a secondary slide. It extends approximately 10 kilometers north of the S4 slide and has a headwall height of approximately 30 meters. In addition to collecting data on the S1 through S5 scarps, the bathymetric data showed a north-south linear depression running subparallel to the continental slope break at the extreme southern end of the S4 escarpment. The Chirp data suggests that "this ~40 km long feature represents the scarp of a previously unrecognized, seafloor breaking normal fault" (Reference 5).

Based on radiocarbon (C-14) analyses of core samples from within 50 kilometers of the slide's headwall, the age of the slide is estimated as between 9 to 14.5 thousand years (References 6 and 7). However, an unconformity occurs between 0.5 and 2 meters depths within the Cape Fear Slide complex. The ages of the samples collected from the cores below the unconformity are older than 29 thousand years. An interpretation of these data indicated a hiatus on the sole of the slide that separated the sediments that are younger than 14.5 thousand years from those that are older than 29 thousand years and that the slide was active during that time (Reference 6). This period of slide activity most likely occurred at the transition between the end of the last glaciation (Wisconsinan Stage) and

the present interglacial age. This age bracket appears to be associated with the Pleistocene sea level lowstand between approximately 12,000 and 28,000 years during the last glacial maximum (References 3, 4, 5, 6, 7, 8, 9 and 10). The possible triggering mechanisms for the slide activity are salt movement, driven by sediment loading, with salt diapirism causing over steepening of the seabed slope followed by failure and potential sediment instability due to gas hydrate decomposition (References 3, 5, 8, 10 and 11).

Representation of the Cape Fear Slide in the Model

The maximum potential slide at Cape Fear was schematized for modeling purposes as having a Gaussian shape with an elliptical footing that extends from the uppermost head scarp to the salt diapirs in the downslope region. This shape was chosen because a Gaussian shape has been used for several investigations and studies of landslide tsunamis, including benchmark cases (References 14, 19, 21). Grilli and Watts (Reference 14) state that a Gaussian shape is a more realistic representation of a submarine mass failure than other arbitrary fixed shapes. Enet & Grilli (Reference 12) used a Gaussian shape in the experiments that provide the basis for the validation of the model used to simulate the generation of a wave by a submarine slide (Reference 12). The Gaussian shape of the slide was approximated in the numerical model by truncated hyperbolic secant squared functions (Reference 12). The center of the elliptical base of the slide was initially located near the S1 headwall in Figure 2 of Reference 5, at 33.14°N, 76.29°W. This location places the uppermost end of the slide area at a depth of approximately 710 meters.

The length (minor axis of the elliptical base) of the slide is approximately 38 kilometers, based on the distance from the upper scarp (described as S1 in Reference 5 and as upper headwall scarp in Reference 1) to the salt diapirs downslope shown in Figure 2 of Reference 5. This represents a conservative upper bound for the length of a potential slide. The width (major axis of the elliptical base) of the slide was assumed to be approximately 50 kilometers, taken conservatively from the width of the largest scarp, S4 (the main scarp). The use of 50 kilometers as the width of the slide is conservative as it is five times the width of the upper scarp (reported as 10 kilometers in Reference 5) where the initial centroid of the postulated slide is assumed.

The thickness of the postulated slide was taken as approximately 120 meters. This is equal to the maximum thickness of the main scarp of the Cape Fear slide, S4, located at 2300 meters depth and is larger than the thicknesses of all the other scarps. For instance, the height of the uppermost scarp at 890 meters depth is much smaller, at about 20 meters (Reference 13). Using a slide thickness of 120 meters is therefore a conservative assumption because the centroid of the postulated slide for the tsunami simulations is placed near the uppermost scarp, S1, at much smaller depth than the lower scarp of the Cape Fear slide. The assumed dimensions and shape of the postulated slide give an area of 1492 km^2 for the base of the slide and a total volume of 68 km^3.

The bottom slope used was 3.09° based on a measured depth difference of 1350 meters over a distance of 25 kilometers in the area of the downslope movement of the slide. The distance of 25 kilometers is based on the presence of a slope break in the Cape Fear profile at about 25 kilometers from the initial location of the centroid, after which the slope decreases by approximately one-half. The direction of the downslope movement of the

slide forms a 10° angle clockwise with the West-East direction. This direction is based on the delineation and orientation of the Cape Fear slide from the GLORIA mapping data.

The initial acceleration of the slide, 0.529 m/s^2, is estimated directly from the bed slope. The terminal velocity of the slide was estimated using Equation (10) in Reference 12 as equal to 138 m/s. As stated earlier, this estimate was obtained using a specific gravity for the slide equal to 2 (Reference 5), and a bed slope of 3.09° and a slide length of 38 kilometers. The global drag coefficient was assumed to be 1 (Reference 14), which is conservative. Based on its initial acceleration the slide reaches its terminal velocity within 260 seconds.

Initial Wave Generated by the Cape Fear Slide

Two alternative approaches were used for the generation of the initial wave in the tsunami simulations. The two approaches are referred to as the dynamic source approach and the static source approach. Two source approaches are used as the velocity components from the dynamic source can differ significantly from the static source with respect to the total slide energy.

The dynamic source approach defined the initial condition for the tsunami propagation simulations in terms of both the water surface displacement and the depth-averaged horizontal velocity fields. This source was computed from the slide geometry and its movement using the computer model NHWAVE (Non-Hydrostatic Wave) (Reference 20). NHWAVE solves the fully non-hydrostatic Navier-Stokes equations in the sigma coordinate system. The model assumes a single-valued water surface and represents turbulent stresses in terms of an eddy viscosity closure scheme. Turbulent stresses are not modeled in the Cape Fear Slide simulation, and thus the model is basically solving the Euler equations for incompressible flow with a moving surface and bottom.

Input to NHWAVE includes the bathymetric grid, the slide dimensions, the initial slide position and orientation, and the terminal velocity. The modeled domain was set up so that the landslide event was centrally located and the generated motion did not reach the lateral boundaries during the simulated time. Bathymetric data for the model domain of NHWAVE and the three nested grids of FUNWAVE-TVD used in the simulations were obtained from the National Geophysical Data Center (NGDC) ETOPO 1 (Reference 22) and the Coastal Relief Model (CRM) (Reference 23) data sets. Results from the NHWAVE model output at 500 seconds after the initiation of the slide were saved and used as initial conditions in the tsunami propagation model FUNWAVE-TVD. The reason for selecting the NHWAVE solution at 500 seconds as input to the tsunami propagation model, was that at that time the maximum wave height is about equal to the maximum thickness of the slide (120 meters). After 500 seconds, the NHWAVE model produces wave heights greater than the maximum thickness of the slide, which would be overly conservative.

At 500 seconds, the slide volume moves downslope 64.6 kilometers, i.e., a distance equal to 1.7 times the length of the minor axis of the elliptical base of the slide, which is aligned with the direction of downslope movement (38 kilometers). The present approach neglects the spreading and flattening of the sliding mass during the slide process. This results in a higher and narrower initial elevation hump at the final slide location than what would have occurred if the slide were allowed to deform. The initial

and final positions of the slide are displayed in Figure 2. The water depth at the initial location of the centroid of the slide is 1100 meters. The water depth at the final position of the centroid of the slide is 3300 meters (Figure 2).

The resulting water surface displacement from NHWAVE at that time (500 seconds) is shown in Figure 3 and Figure 4, which also shows the water surface profile in the direction of the slide motion simulated with NHWAVE at different times after the initiation of the slide. As shown in Figure 4 the maximum water surface at 500 seconds is 122 meters, and the minimum –166 meters.

The second approach to the generation of the initial condition for the tsunami propagation model used a static source based on the geometry of the initial and final positions of the slide mass. A static source is defined as an initial displacement of the water surface in the form of a depression over the initial slide location, equal in areal extent, shape and volume to the displaced material volume during the submarine slide. It was assumed that the initial slide volume described above translates downslope along its axis in the direction of the slope beyond its original footprint. A positive displacement of the water surface equal to the volume, shape and size of the slide was assumed at that point, i.e., extending over an elliptical area with minor axis equal to 38 kilometers, major axis 50 kilometers and maximum thickness 120 meters, and a corresponding negative displacement representing the missing volume of the slide mass was added at the slide starting point. The centroid of the depression of the water surface was placed at 33.14°N, 76.29°W, same as the initial location of the centroid of the slide for the dynamic source. A water rise equal in shape and size with the depression was assumed downslope of the initial depression and at a distance equal to translation distance of the dynamic case, i.e., 64.6 kilometers. The maximum water surface rise is equal to 120 meters. Figure 5 shows the assumed initial water surface wave for the Cape Fear tsunami simulation with FUNWAVE-TVD based on a static source. Using an initial static source, it was assumed that the initial horizontal velocities were zero over the entire model domain of FUNWAVE-TVD.

Modeling of Tsunami Propagation and Inundation

The propagation, shoreline runup and inundation caused by the Cape Fear tsunami were simulated using the Boussinesq wave model FUNWAVE-TVD, developed at the University of Delaware. In its present application, FUNWAVE-TVD solved the spherical-polar form of the weakly-nonlinear, weakly-dispersive Boussinesq equations described in Reference 16. Reference 17 describes the operation of both Cartesian and spherical-polar versions of the code. The model incorporates bottom friction and subgrid lateral turbulent mixing effects.

The Cartesian coordinate version of FUNWAVE-TVD, described in References 17 and 18, has been validated using several PMEL-135 benchmarks (Reference 19), which are the presently accepted benchmarking standards adopted by the National Tsunami Hazard Mitigation Program (NTHMP) for judging model acceptance for use in development of coastal inundation maps and evacuation plans. Benchmark tests for the Cartesian version of FUNWAVE-TVD are described in Reference 17. Benchmark tests for the spherical version of the code are described in Reference 16.

The equations solved by FUNWAVE-TVD consist of a depth-integrated volume conservation equation together with depth-integrated horizontal momentum equations. These equations are summarized in References 17 and 18. For tsunami applications, FUNWAVE-TVD is run with closed boundaries and an initial hot start condition consisting of either a surface displacement alone (in the case of static initial conditions) or a surface displacement and initial velocity field (in the case of a dynamic initial condition based on the results of calculations with NHWAVE). The model is run from the initial start until past the time when significant wave activity has decayed at the target site.

In most large scale problems, FUNWAVE-TVD is run on more than one nested grid. The grid nesting scheme uses a one-way nesting technique, which passes surface elevation and velocity components calculated from a large domain to a nested small domain through ghost cells at nesting boundaries. A linear interpolation is performed between the large and the small domain at the nesting boundaries. A test of the nesting process is included in the FUNWAVE-TVD verification and validation document (Reference 16).

In the simulations of the Cape Fear tsunami, three nested grids are used, which are referred to as Grid A, Grid B, and Grid C. The output from Grid A is input to FUNWAVE-TVD on Grid B. The same process is repeated in going from Grid B to Grid C.

The domain covered by each of these three grids is shown in Figure 6. All the grids are based on geographic coordinates. The coordinates of the southwest corner of each grid, the grid spacing and number of grid cells in each grid are given in Table 1.

Table 1. Nested grids used in FUNWAVE-TVD

Grid	Coordinates of SW Corner		Grid Spacing ($\Delta x = \Delta y$)	Number of Grid Cells
	x	y		
	degrees	degrees	seconds	cells
A	-82.0	23.0	60	780 x 900
B	-80.75	23.0	15	480 x 1260
C	-80.517	25.322	3	592 x 768

It is noted that because of the curvature of the earth, having a uniform grid size in degrees leads to variable-length (in the west-east direction) cells at different latitudes within the model domain.

There is a sponge layer along the open boundaries of the model which was used for the definition of the boundary conditions. The thickness of the sponge layer was 200 kilometers along the eastern boundary, and 100 kilometers along the northern and southern boundaries.

The antecedent water surface level used for the model simulation was equal to the 10% exceedance spring tide level, plus the initial rise and long term sea level rise, which produce an initial water level equal to 1.68 meters (5.5 feet) mean low water (MLW), or 3.6 feet (1.10 meters) NAVD 88, same as that used for the PMT numerical simulation in FSAR 2.4.6.4 and for the probable maximum storm surge evaluation as explained in FSAR 2.4.5.2.2.1.

Simulation Results

Two sets of simulation results for the tsunami propagation and inundation by the Cape Fear tsunami are presented. The first set of results is for the dynamic initial condition and the second is for a static initial condition.

Dynamic Source Initial Condition

Figure 7 and Figure 8 show the propagation of the tsunami wave over the domain of model Grid A during the first three hours of the FUNWAVE-TVD simulation, presenting snapshots of the wave height every 20 minutes. Time zero in the FUNWAVE-TVD simulation is 500 seconds after the initiation of the slide It should be noticed that the color scale indicating wave height differs in the different panels of these two figures. As can be seen in these figures, the highest waves travel towards the east. The wave traveling west towards the east coast of the United States is relatively smaller. Relatively high water levels are also predicted towards the southeast. This is illustrated in Figure 9 which shows the maximum water surface elevation within the model domain of Grid A during the simulation period. The highest water levels are within a fan-shaped zone towards the east, and over a relatively narrow zone towards the southeast. The latter seems to coincide with the relatively shallower ocean depths along Blake Ridge (Figure 6).

Figure 10 shows the propagation of the tsunami wave in Grid B, from 100 minutes in the FUNWAVE-TVD simulation, a little after the wave enters the Grid B domain, until 180 minutes. Snapshots of the wave height every 20 minutes are shown. Figure 11 shows the maximum water surface elevation within the model domain of Grid B during the simulation period. As can be seen in this figure, the highest water levels occur in the northern part of Grid B, while the water levels toward the south and in the vicinity of Units 6 & 7 are much lower.

Figure 12 shows the propagation of the tsunami wave in Grid C, from 140 minutes until 240 minutes in the FUNWAVE-TVD simulation. Snapshots of the wave height every 20 minutes are shown. Figure 13 shows the maximum water level over Grid C. As can be seen in these figures, the area surrounding the site of Units 6 & 7 is inundated. However, the Units 6 & 7 site itself and other parts of the Turkey Point station, which are elevated above the existing grade, are not inundated and remain dry. The inundation of the area surrounding the site of Units 6 & 7 is not caused by the Cape Fear tsunami. It is a consequence of the assumption regarding the initial sea water level rise which accounts for the 10% exceedance spring tide level, 3.6 feet mean low water (MLW), initial rise, 0.9 feet and long term sea level rise, 1.0 foot, which produce an initial water level, i.e., prior to the arrival of the tsunami, equal to 1.68 meters (5.5 feet MLW), or 3.6 feet (1.10 meters) NAVD 88. This initial water level is enough to inundate a large zone along the Florida coast, including the entire area around Units 6 & 7. This is made clear in Figure 14, which shows the water depth over the area of Grid C relative to two different levels of the water surface. The left panel shows the water depth relative to MLW. The right panel shows the water depth relative to the assumed initial water surface in the Cape Fear tsunami simulations, i.e., relative to MLW + 10% exceedance spring tide + initial rise + long-term sea level rise. As can be seen in the right panel of Figure 14, the area surrounding the site of Units 6 & 7 and its vicinity are inundated even prior to the arrival of the tsunami. Again, the Units 6 & 7 site itself and other parts of the Turkey Point station,

which are elevated above the existing grade, are not inundated and remain dry. Figure 15 shows the maximum water surface rise in the vicinity of Units 6 & 7, relative to the initial sea water level. The maximum water surface elevation at the Turkey Point Power Station is 2.28 meters (7.5 feet) MLW, or 5.7 feet (1.75 meters) NAVD 88.

Figure 16 shows the water level near Units 6 & 7 from the dynamic source simulation as a function of time. The maximum water surface level rise caused by the Cape Fear tsunami is 0.6 meters over the initial water level, occurring a little after five hours from the initiation the Cape Fear slide, and about two hours after the arrival of the first waves caused by the Cape Fear tsunami.

Static Source Initial Condition

Figure 17 and Figure 18 show the propagation of the tsunami wave generated by a static source over the domain of Grid A during the first three hours of the FUNWAVE-TVD simulation, presenting snapshots of the wave height every 20 minutes. The tsunami propagation pattern is similar to that in the dynamic source simulation, but the wave heights away from the source, especially towards the east are much smaller than those for the dynamic sources shown in Figure 7 and Figure 8.

Figure 19 shows the maximum water surface elevation within the model domain of Grid A during the simulation period. Comparing Figure 19 with Figure 9 shows that the static source produces much smaller water surface elevations over most of the domain of Grid A, and especially to the east and southeast. An exception is the area right over the slide and its immediate vicinity to the west, where the maximum water surface levels with the static source are substantially higher than those obtained with the dynamic source. This could be attributed to the fact that in the case of the dynamic source the initial condition entered in FUNWAVE-TVD includes the velocities obtained with NHWAVE, while in the case of the static source the initial velocities in the vicinity of the source are zero. Assigning a velocity to the initial wave in the dynamic source case results in a higher total energy than in the static source case where the initial velocity is assumed to be zero.

Figure 20 shows the propagation of the tsunami wave in Grid B, from 100 minutes in the FUNWAVE-TVD simulation, a little after the wave enters the Grid B domain, until 180 minutes. Snapshots of the wave height every 20 minutes are shown. Figure 21 shows the maximum water surface elevation within the model domain of Grid B during the simulation period. The predicted water surface levels in Grid B for the static source are quite similar to those for the dynamic source shown in Figure 10 and Figure 11.

Figure 22 shows the propagation of the tsunami wave in Grid C, from 140 minutes until 240 minutes in the FUNWAVE-TVD simulation. Snapshots of the wave height every 20 minutes are shown. Figure 23 shows the maximum water level over Grid C. Again the predicted water surface elevations over Grid C for the static source are quite similar to those predicted with a dynamic source, shown in Figure 12 and Figure 13.

Figure 24 shows the maximum water surface rise in the vicinity of Units 6 & 7, relative to the initial sea water level. The maximum water surface elevation is 2.08 meters (6.8 feet) MLW, or 5.0 feet (1.51 meters) NAVD 88.

Figure 25 shows the water level near Units 6 & 7 from the static source simulation as a function of time. The maximum water surface level rise caused by the Cape Fear tsunami is 0.4 meters, occurring a little after four hours from the initiation the Cape Fear

slide, and about one hour after the arrival of the first waves caused by the Cape Fear tsunami. The maximum water level near Units 6 & 7 predicted with the static source (0.4 meters) is slightly lower than that predicted using a dynamic source (0.6 meters).

Summary of Results

A literature review was performed to identify the characteristics of a potential future submarine slope failure on the continental margin off Cape Fear. Conservative assumptions were made to define such a submarine slide as a source of a tsunami event. The postulated slide was 38 kilometers long (in the direction of motion), 50 kilometers wide and had a maximum thickness of 120 meters. It was assumed to have an elliptical base with its minor and major axes equal to the postulated length and width.

Simulations with two alternative initial conditions (dynamic and static) for the water surface at the onset of the tsunami event were made. In both cases, the assumed initial sea water level includes the 10% exceedance spring tide, 3.6 feet mean low water (MLW), an initial rise, 0.9 feet, plus the long-term sea level rise, 1.0 foot, all of which add up to 1.68 meters (5.5 feet) MLW, or 3.6 feet (1.10 meters) NAVD 88. This assumption leads to inundation of large parts of southeast Florida, including the area around Units 6 & 7 even prior to the arrival of the Cape Fear tsunami.

First, the non-hydrostatic code NHWAVE was used to simulate the motion of the slide and generate the water surface elevation and horizontal velocities used as the dynamic source initial conditions in the simulation of the tsunami propagation with the Boussinesq code FUNWAVE-TVD. The initial maximum wave and negative (depression) wave produced by NHWAVE were 122 meters and -166 meters, respectively. The propagation of the tsunami was simulated through three nested grids (Grid A, Grid B, and Grid C), each of which provided finer grid resolution. The simulation suggests that the relative water surface rise near Units 6 & 7 due to the Cape Fear slide is small. The predicted maximum water surface elevation is 2.28 meters (7.5 feet) MLW or 5.7 feet (1.75 meters) NAVD 88, representing a rise of 0.6 meters relative to the assumed initial sea water level of 1.68 meters (5.5 feet) MLW, or 3.6 feet (1.10 meters) NAVD 88.

Secondly, a static source approach was used. In this case, the initial condition for the tsunami wave was assumed to be a dipole with a depression and a rise of water levels having the shape of the displaced mass of the submarine failure. The initial water surface condition for the FUNWAVE-TVD simulations includes a 120-meter depression of the water surface over the slide and a 120-meter rise downslope of the slide. The initial velocity field in this case is zero. The predicted water levels with the static source are lower to the east and southeast, but higher over the slide area and its vicinity to the west. The predicted water levels near Units 6 & 7 were quite similar to those obtained with the dynamic source. The predicted maximum water surface elevation near the site is 2.08 meters (6.8 feet) MLW, or 5.0 feet (1.51 meters) NAVD 88, representing a rise of 0.4 meters above the initial sea water level.

Conclusions

Simulations of a tsunami generated by a conservatively large submarine mass failure on the continental margin off Cape Fear suggest that the impact of such an event on water levels near Units 6 & 7 will be small. The maximum predicted water level due to the tsunami event will be 2.28 meters (7.5 feet) MLW, or 5.7 feet (1.75 meters) NAVD 88, representing a rise of 0.6 meters of the initial sea water level. The assumed initial sea water level includes the 10% exceedance spring tide, an initial rise plus the long-term sea level rise. This water level is much smaller than the maximum tsunami water level of 4.5 meters MSL (4.82 meters MLW) reported for the PMT case in FSAR Subsection 2.4.6.5. This conclusion is with consistent the results of the Cape Fear Slide evaluation described in FSAR 2.4.6.1.1.

Figure 1. GLORIA side-scan sonar image of the Cape Fear Slide (Source: Reference 1).

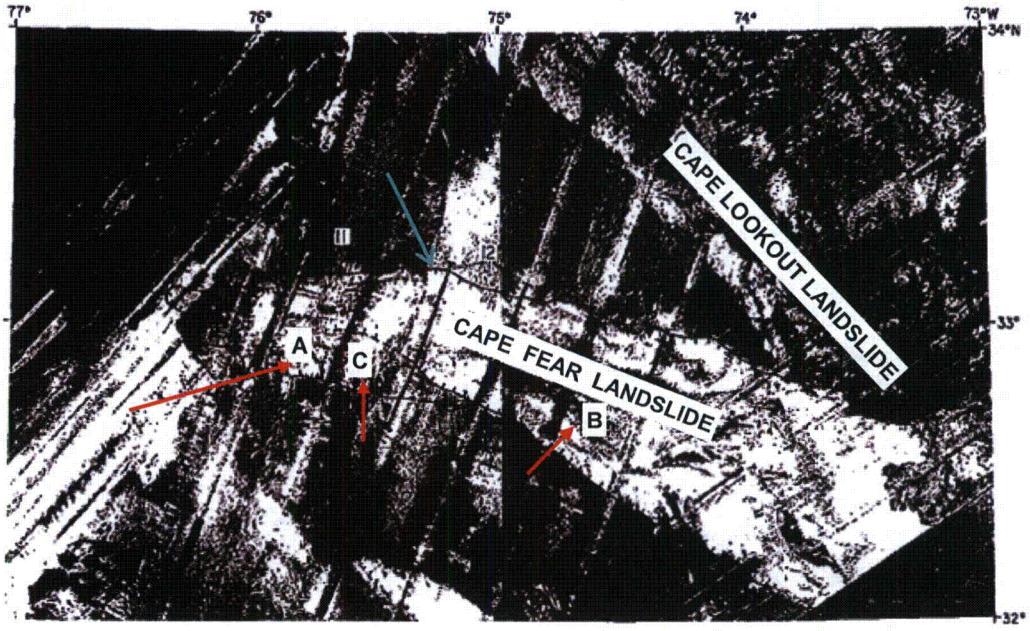

Note: Hachures pointing downslope represents scarps. The lighter acoustic return seen in the image represent mass movement deposits and the dark return are the undisturbed sedimentary deposits. The location (A) represents the longitudinal lines representing both debris chutes between the salt diapirs at the head of the landslide area, and flow paths of debris further down slope, which is shown with location (B). Location (C) is an area of irregular, hummocky sea floor that has been crumpled and buckled by mass movement near the head of the slide. The blue arrow indicates the northern limit of the Cape Fear landslide.

Figure 2. Location and lateral extent of the postulated submarine mass failure for the Cape Fear simulations and local bathymetry. Bathymetry contours indicate water depths (MSL).

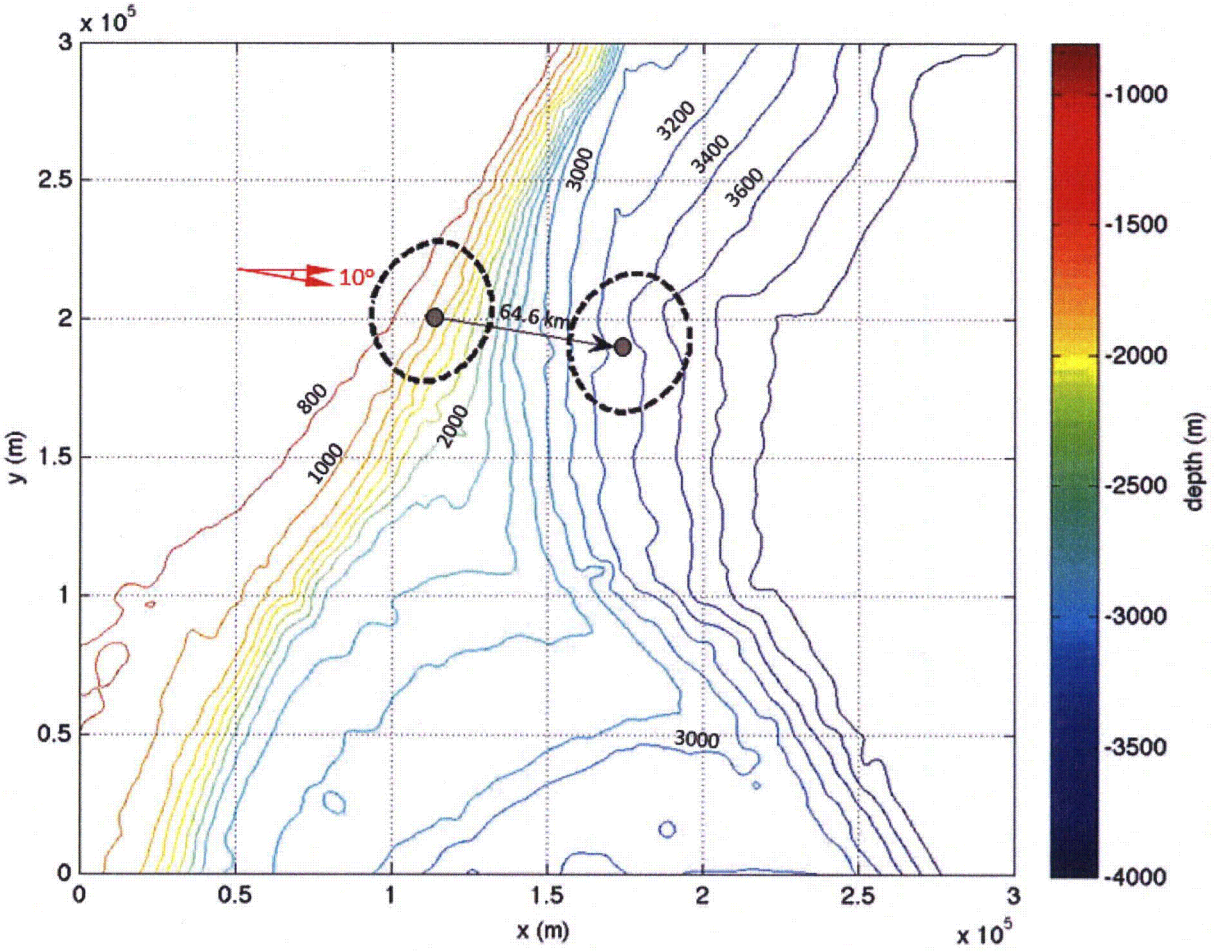

Figure 3. Initial wave generated by NHWAVE (dynamic source) for the Cape Fear submarine failure shown in Figure 2. Colors in elevation legend indicate water surface elevation (MSL) in meters. Bathymetry contours indicate water depths (MSL).

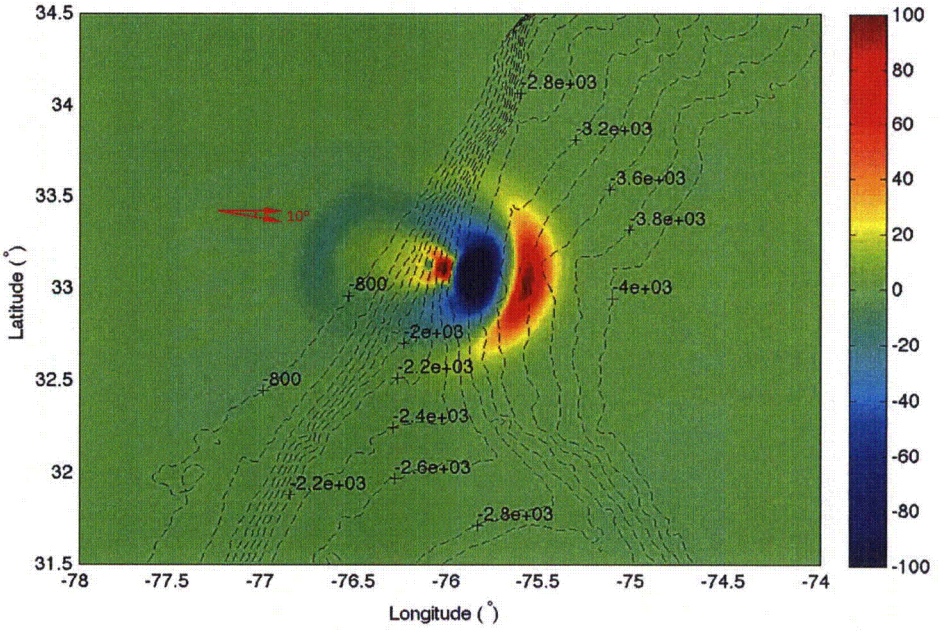

Figure 4. Water surface profile in the direction of the slide motion at different times after the initiation of the slide (upper panel) and ocean floor profile (lower panel). Water surface elevations (upper panel) and water depths (lower panel) are relative to MSL.

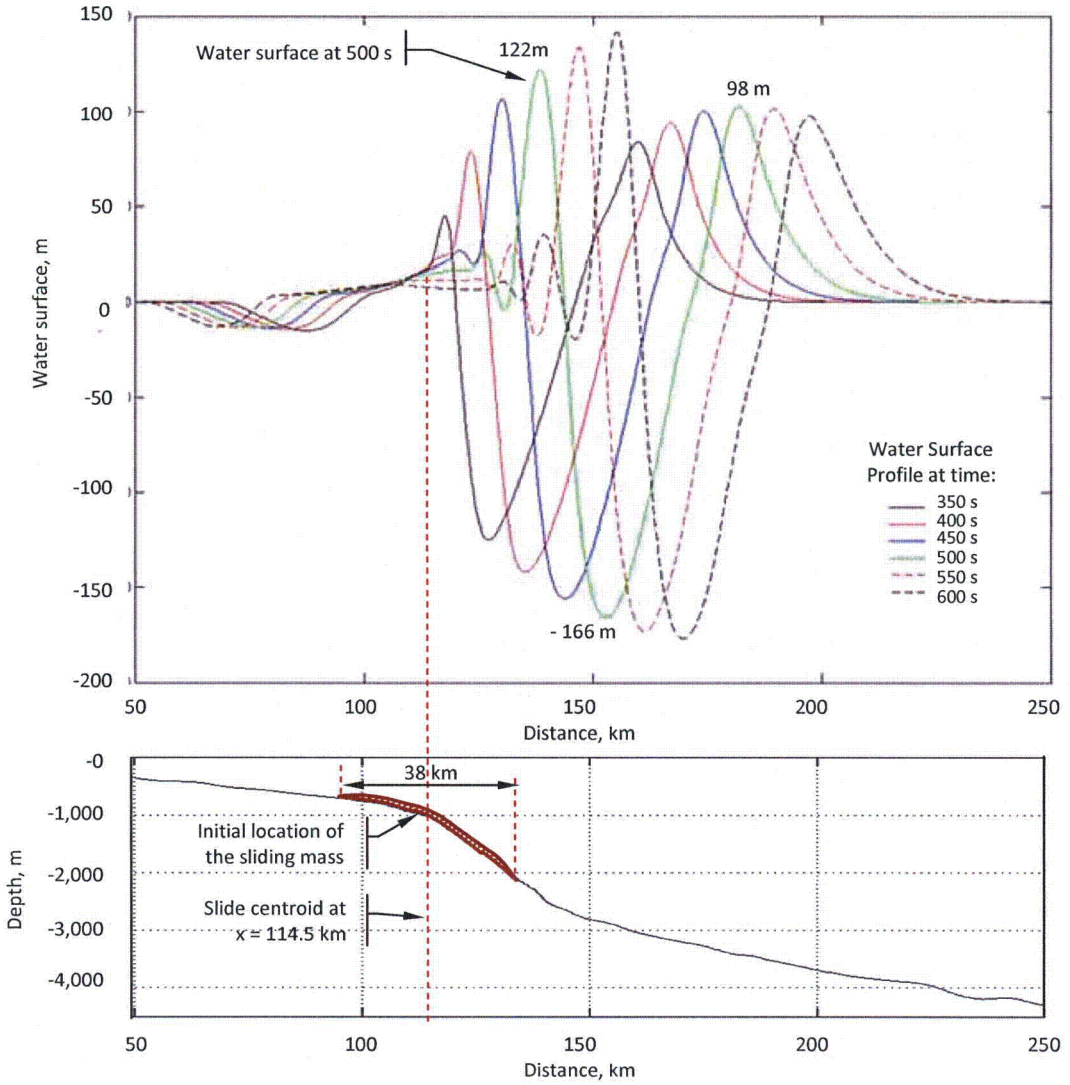

Figure 5. Initial wave for a static source representation of the Cape Fear submarine failure shown in Figure 2. Colors in elevation legend indicate water surface elevation (MSL) in meters. Bathymetry contours indicate water depths (m MSL).

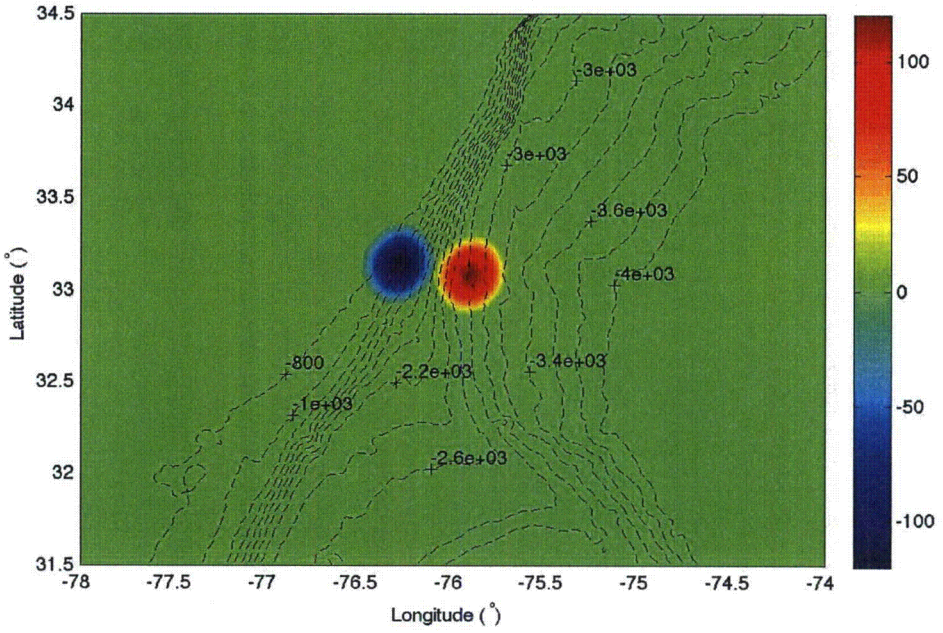

Figure 6. Model domain and bathymetry in the three nested grids used in the FUNWAVE-TVD simulations. Colors in elevation legend represent water surface elevations relative to MSL for ETOPO1 data and MLW for Coastal Relief Model data.

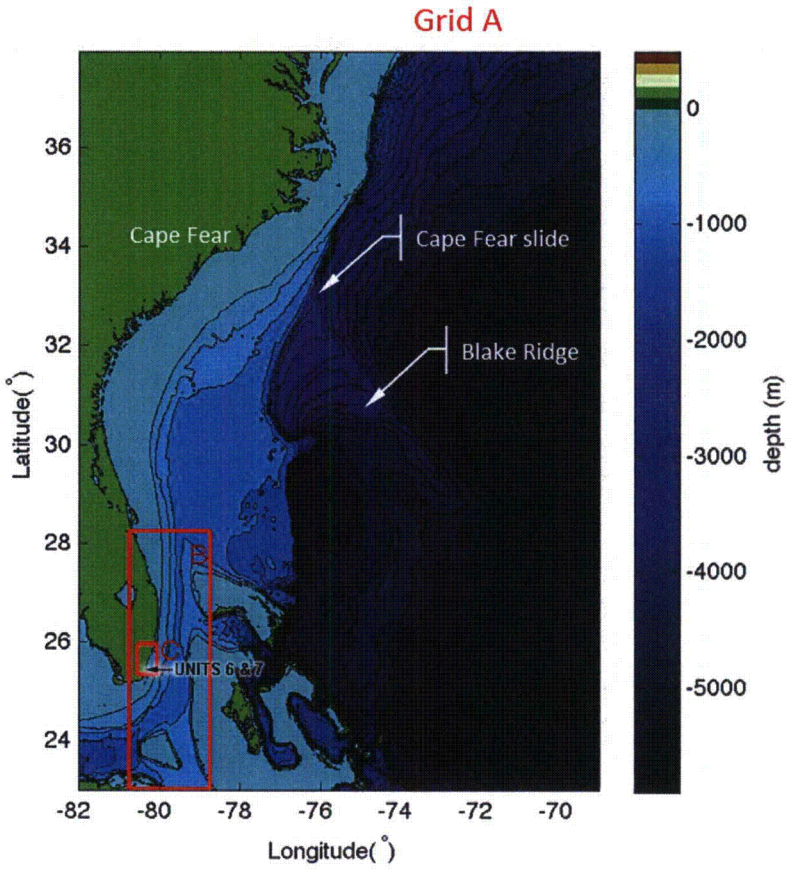

Figure 7. Simulated propagation of the Cape Fear tsunami (dynamic source) in Grid A at 0, 20, 40, 60, 80 and 100 minutes after the submarine failure. Colors in elevation legend represent water surface elevations relative to MSL for ETOPO1 data and MLW for Coastal Relief Model data.

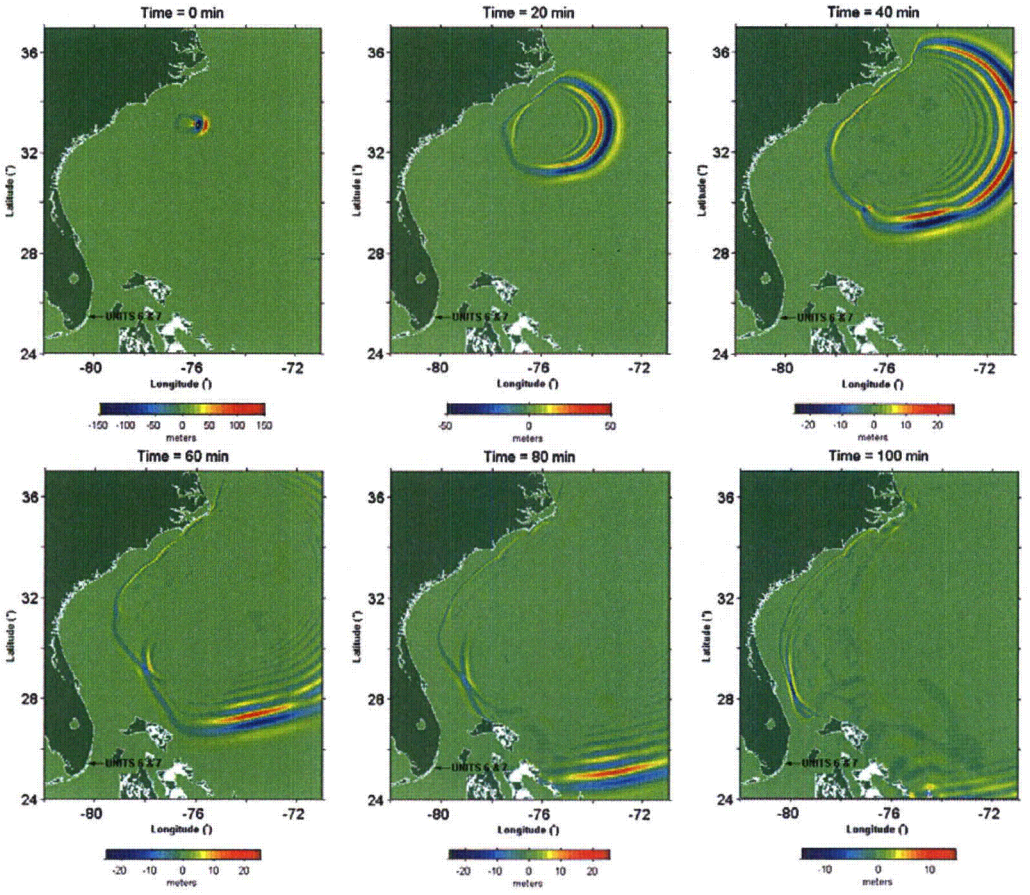

Figure 8. Simulated propagation of the Cape Fear tsunami (dynamic source) in Grid A at 120, 140, 160, and 180 minutes after the submarine failure. Colors in elevation legend represent water surface elevations relative to MSL for ETOPO1 data and MLW for Coastal Relief Model data.

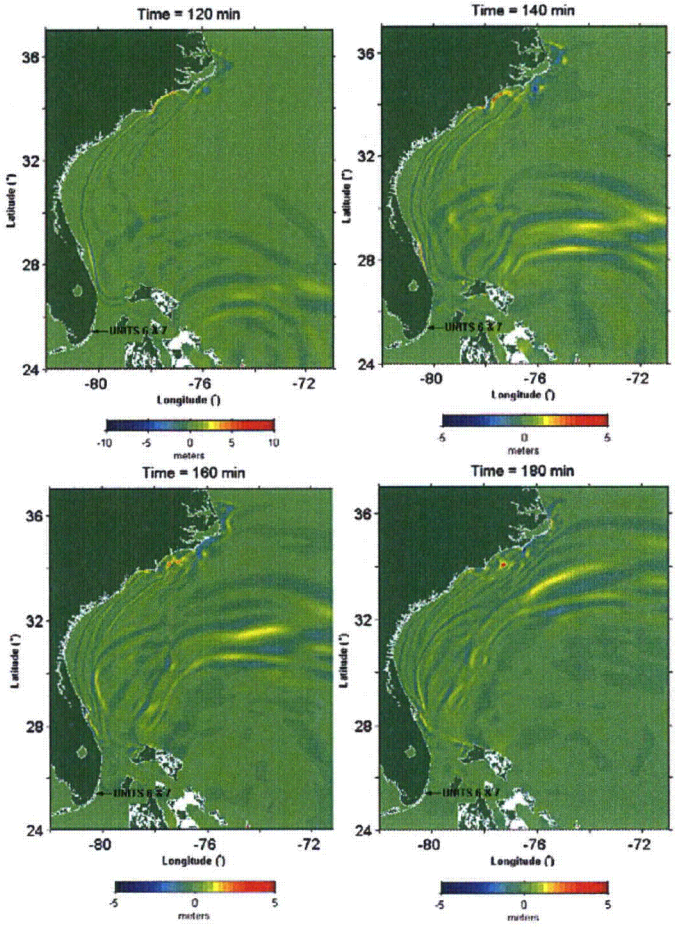

Figure 9. Simulated maximum water surface elevation during the propagation of the Cape Fear tsunami (dynamic source) in Grid A. Colors in elevation legend represent water surface elevations relative to MSL for ETOPO1 data and MLW for Coastal Relief Model data.

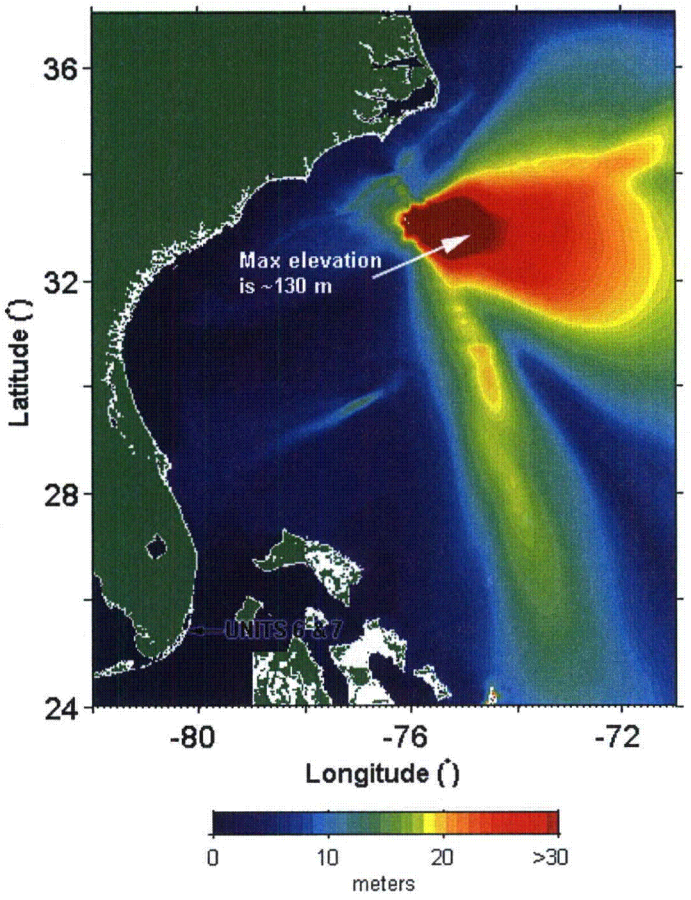

Figure 10. Simulated propagation of the Cape Fear tsunami (dynamic source) in Grid B at 100, 120, 140, 160, and 180 minutes after the submarine failure. Colors in elevation legend represent water surface elevations relative to MSL for ETOPO1 data and MLW for Coastal Relief Model data.

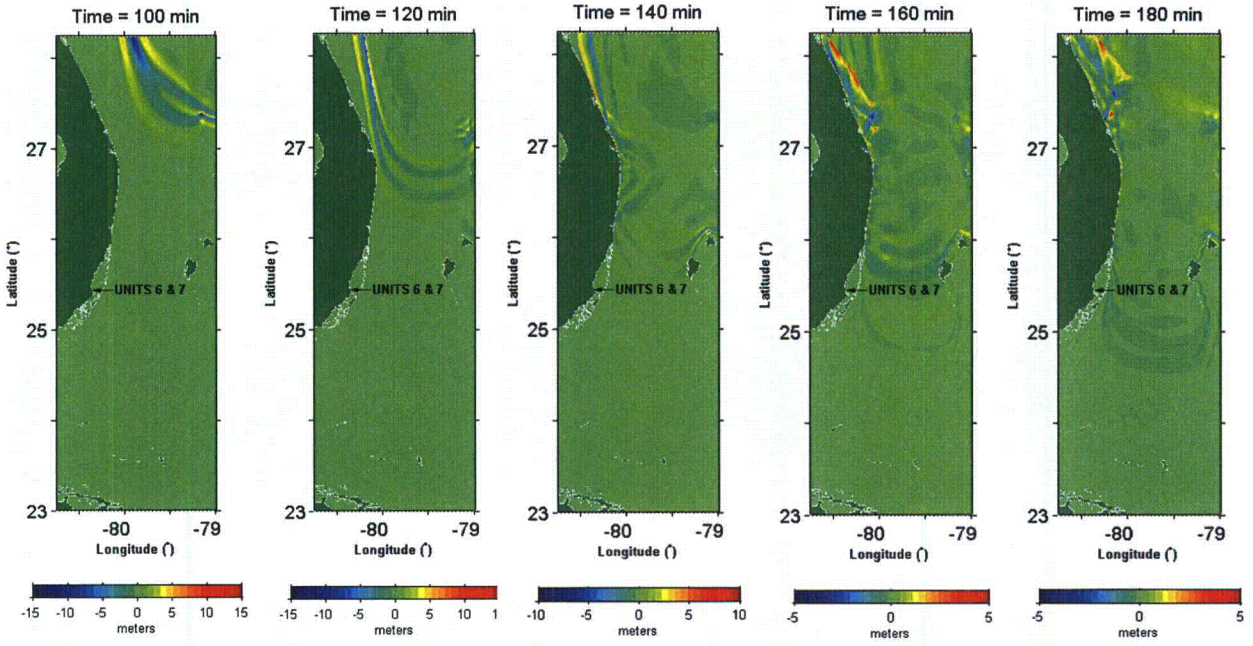

Figure 11. Simulated maximum water surface elevation during the propagation of the Cape Fear tsunami (dynamic source) in Grid B. Colors in elevation legend represent water surface elevations relative to MSL for ETOPO1 data and MLW for Coastal Relief Model data.

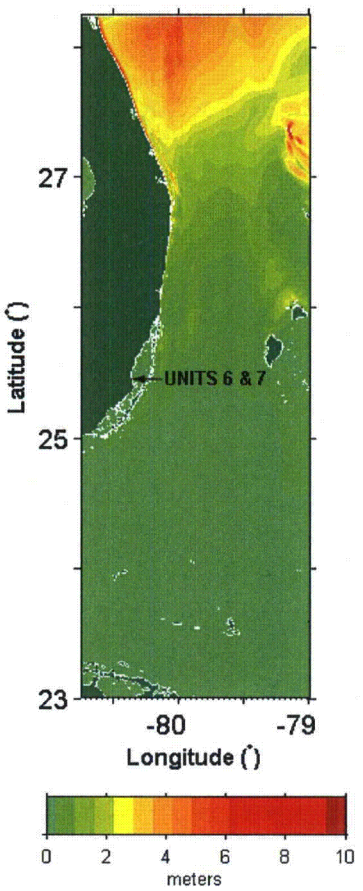

Figure 12. Simulated propagation of the Cape Fear tsunami (dynamic source) in Grid C at 140, 160, 180, 200, 220 and 240 minutes after the submarine failure. Colors in elevation legend represent water surface elevations relative to MLW.

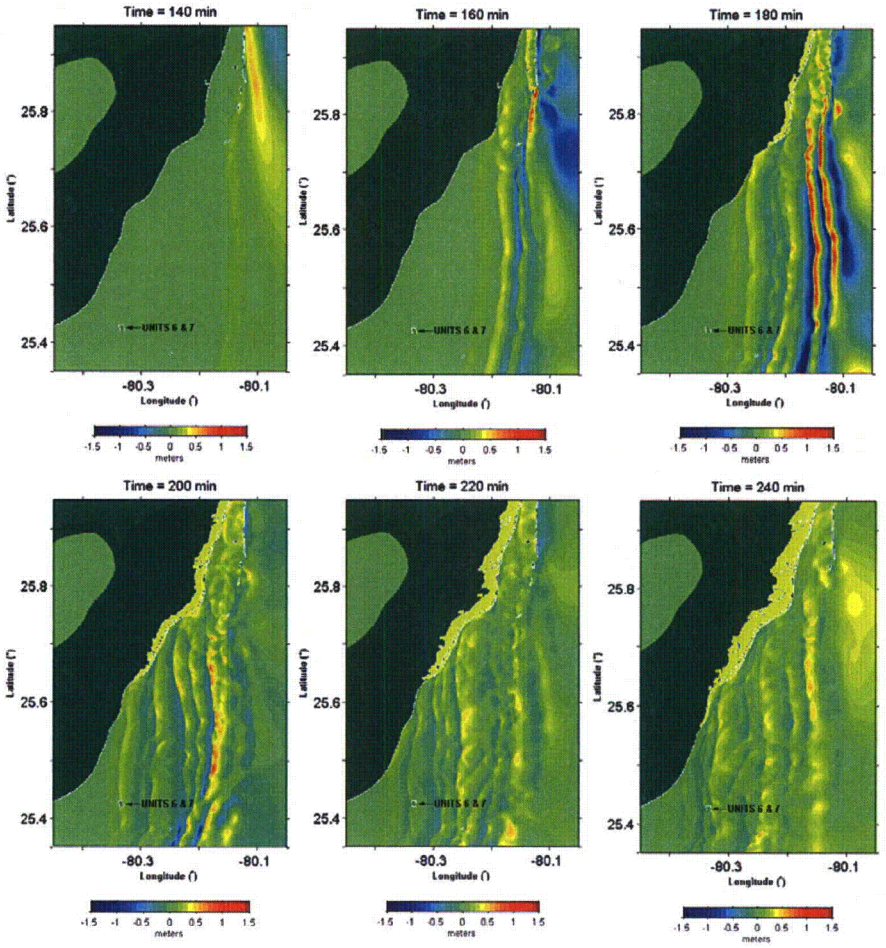

Figure 13. Simulated maximum water surface elevation during the propagation of the Cape Fear tsunami (dynamic source) in Grid C. Colors in elevation legend represent water surface elevations relative to MLW.

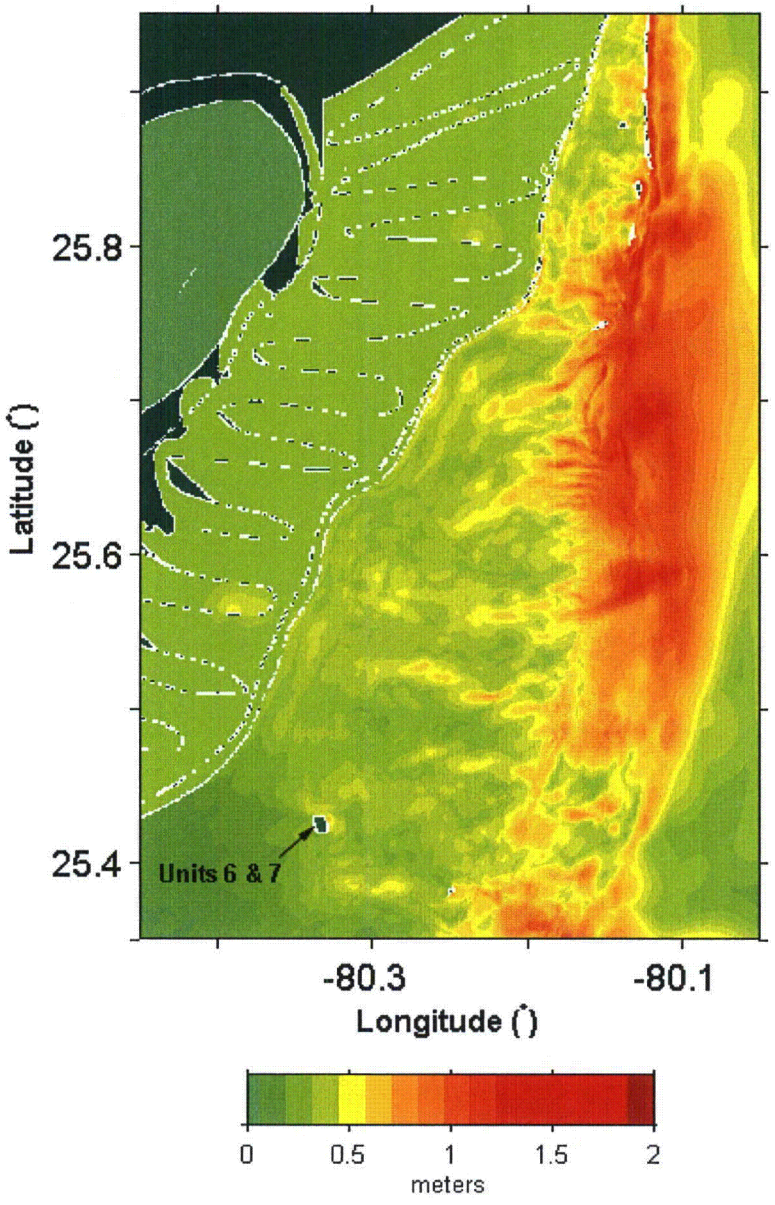

Figure 14. (a) Water depth relative to MLW over the area of Grid C; and (b) water depth relative to the assumed initial water surface in the Cape Fear tsunami simulations, i.e., 10% exceedance spring tide + sea rise + long-term sea level rise. Colors in elevation legend represent water surface elevations relative to MLW.

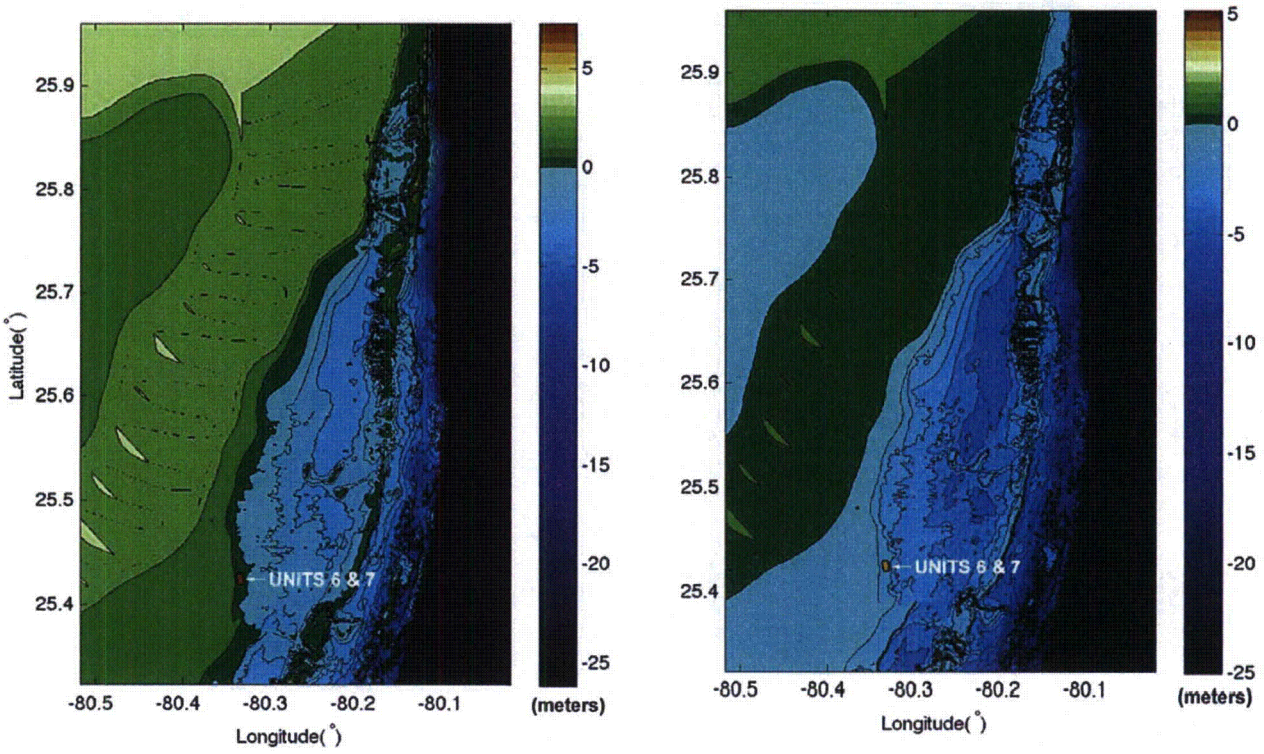

Figure 15. Simulated maximum water surface rise, relative to the initial sea water level, during the propagation of the Cape Fear tsunami (dynamic source) in the vicinity of Units 6 & 7. Colors in elevation legend represent water surface elevations relative to MLW.

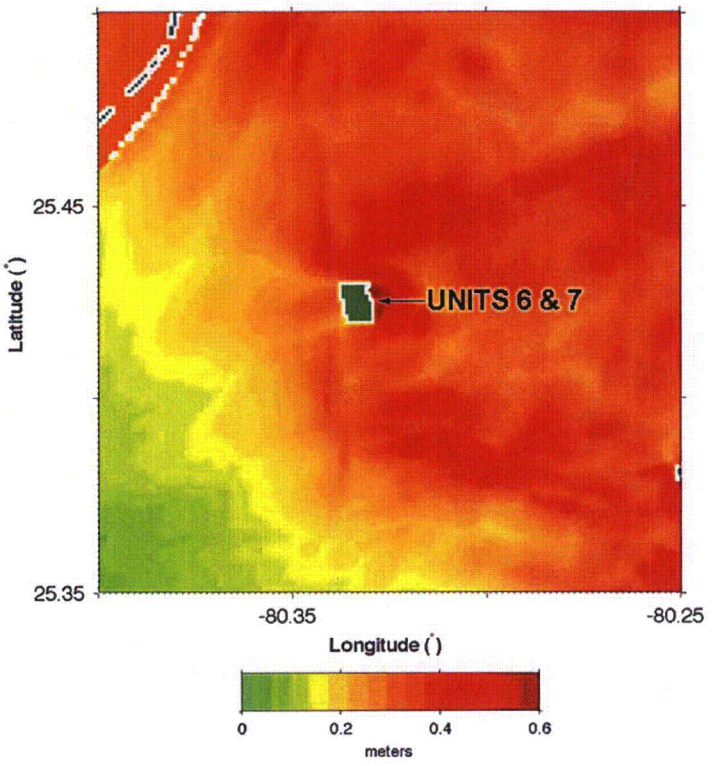

Figure 16. Water surface elevation near Units 6 & 7 as a function of time following the Cape Fear tsunami (dynamic source). Water surface elevations in meters are relative to the initial water level.

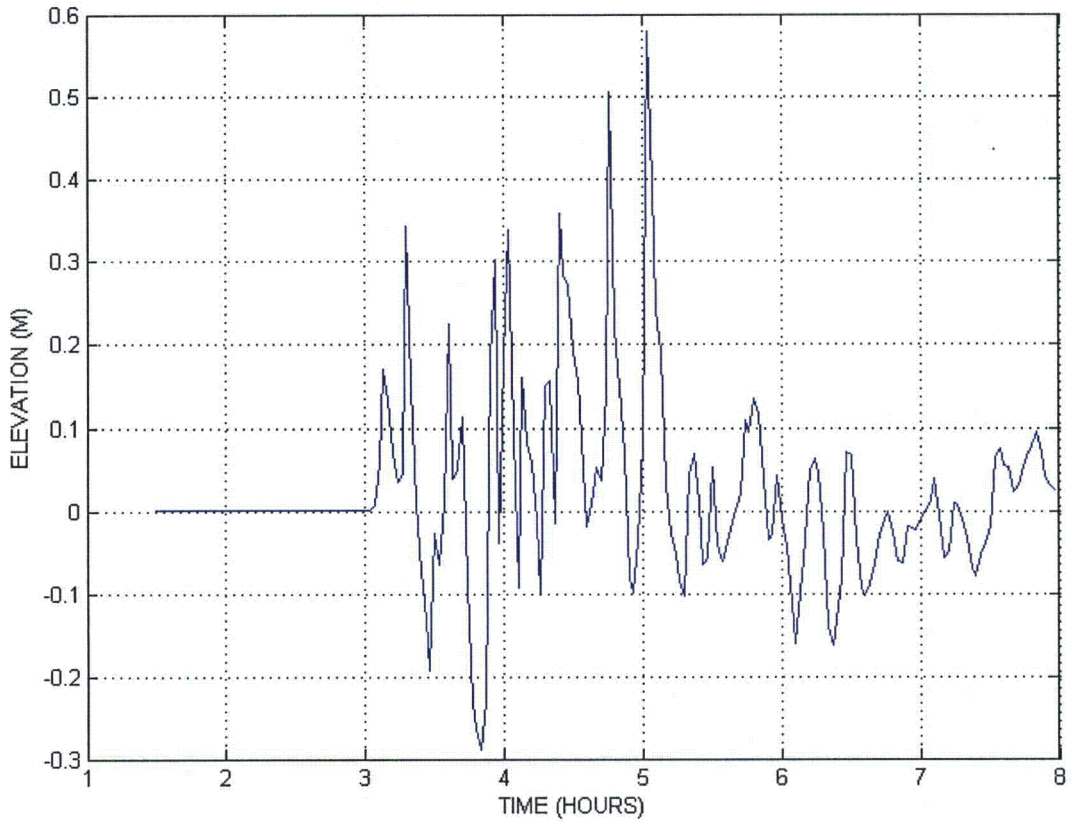

Figure 17. Simulated propagation of the Cape Fear tsunami (static source) in Grid A at 0, 20, 40, 60, 80 and 100 minutes after the submarine failure. Colors in elevation legend represent water surface elevations relative to MSL for ETOPO1 data and MLW for Coastal Relief Model data.

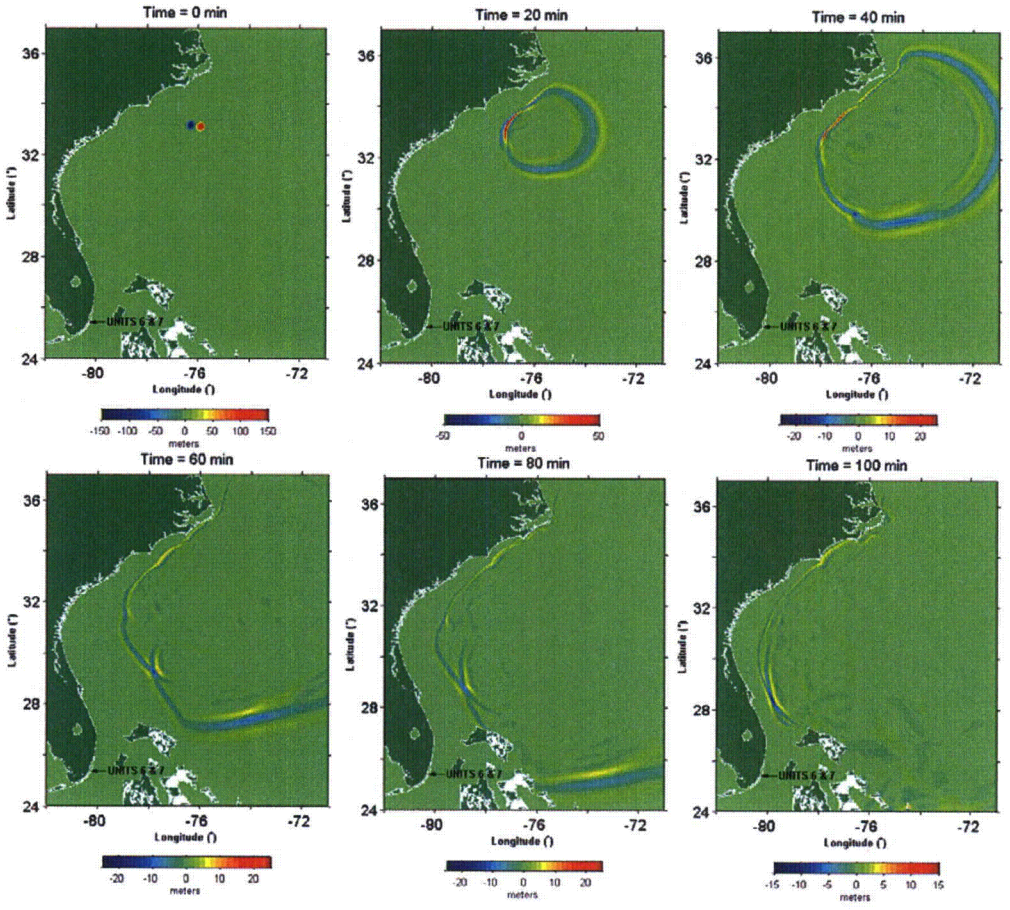

Figure 18. Simulated propagation of the Cape Fear tsunami (static source) in Grid A at 120, 140, 160, and 180 minutes after the submarine failure. Colors in elevation legend represent water surface elevations relative to MSL for ETOPO1 data and MLW for Coastal Relief Model data.

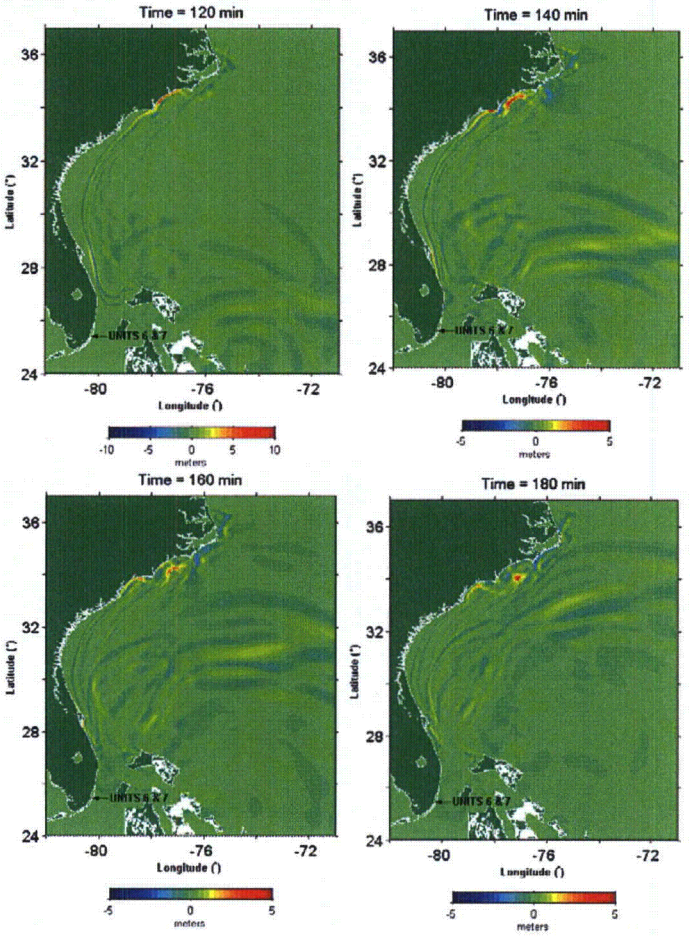

Figure 19. Simulated maximum water surface elevation during the propagation of the Cape Fear tsunami (static source) in Grid A. Colors in elevation legend represent water surface elevations relative to MSL for ETOPO1 data and MLW for Coastal Relief Model data.

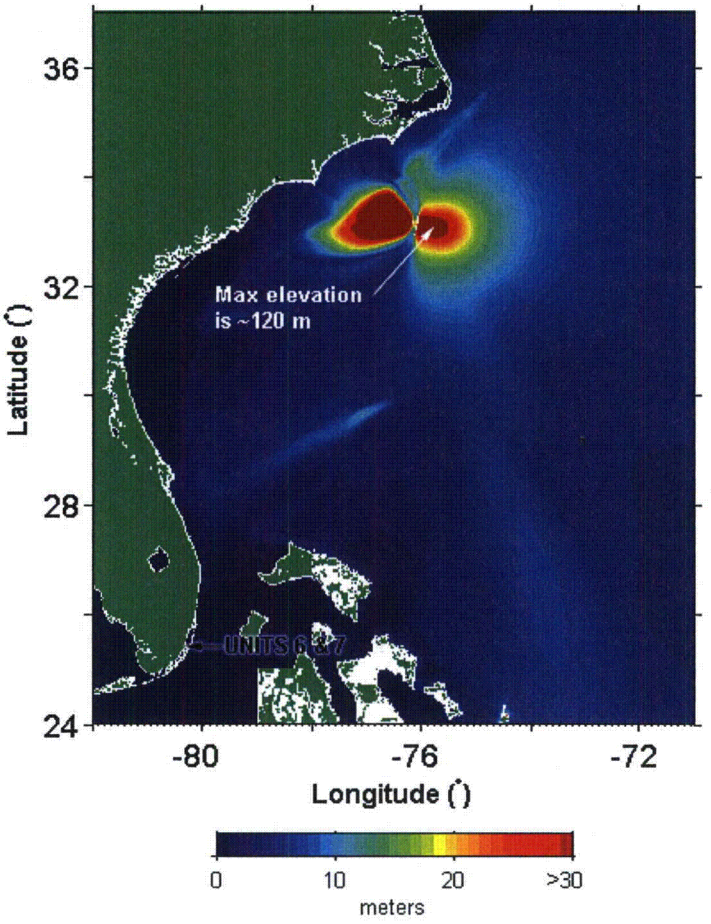

Figure 20. Simulated propagation of the Cape Fear tsunami (static source) in Grid B at 100, 120, 140, 160, and 180 minutes after the submarine failure. Colors in elevation legend represent water surface elevations relative to MSL for ETOPO1 data and MLW for Coastal Relief Model data.

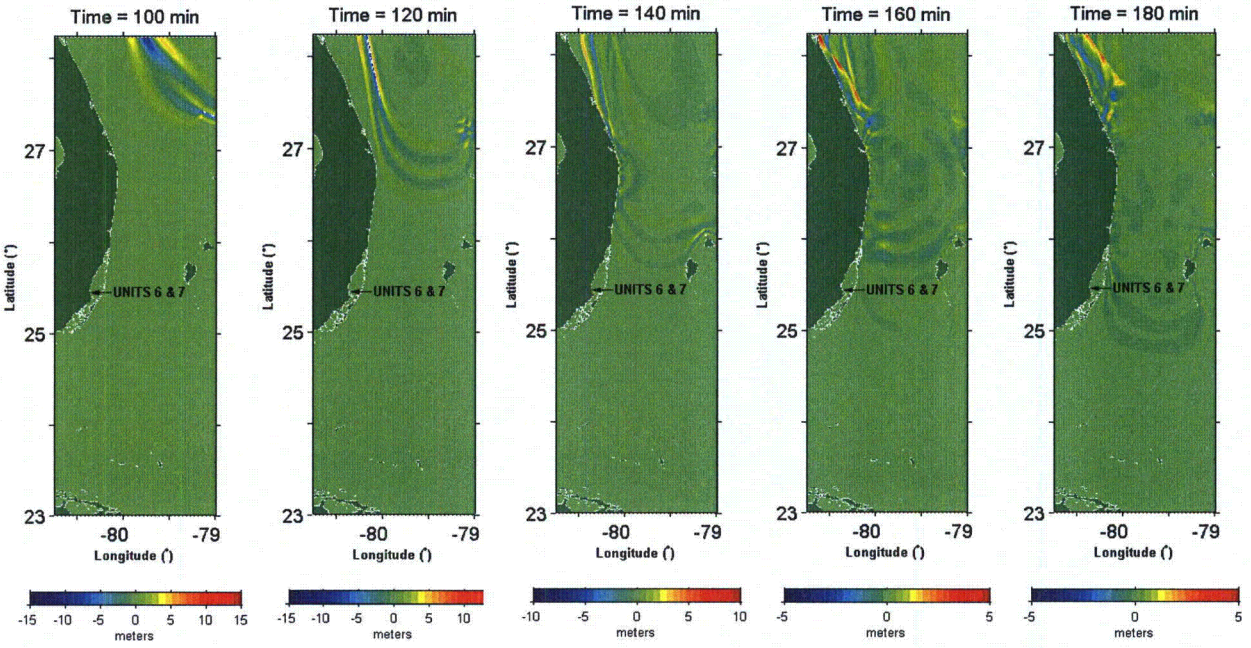

Figure 21. Simulated maximum water surface elevation during the propagation of the Cape Fear tsunami (static source) in Grid B. Colors in elevation legend represent water surface elevations relative to MSL for ETOPO1 data and MLW for Coastal Relief Model data.

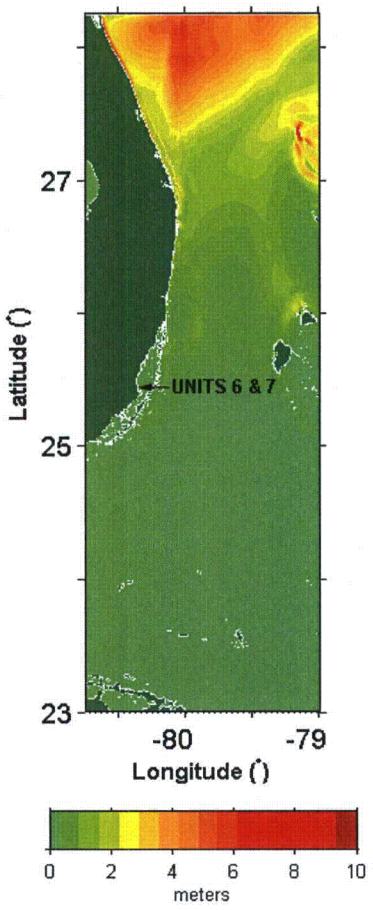

Figure 22. Simulated propagation of the Cape Fear tsunami (static source) in Grid C at 140, 160, 180, 200, 220 and 240 minutes after the submarine failure. Colors in elevation legend represent water surface elevations relative to MLW.

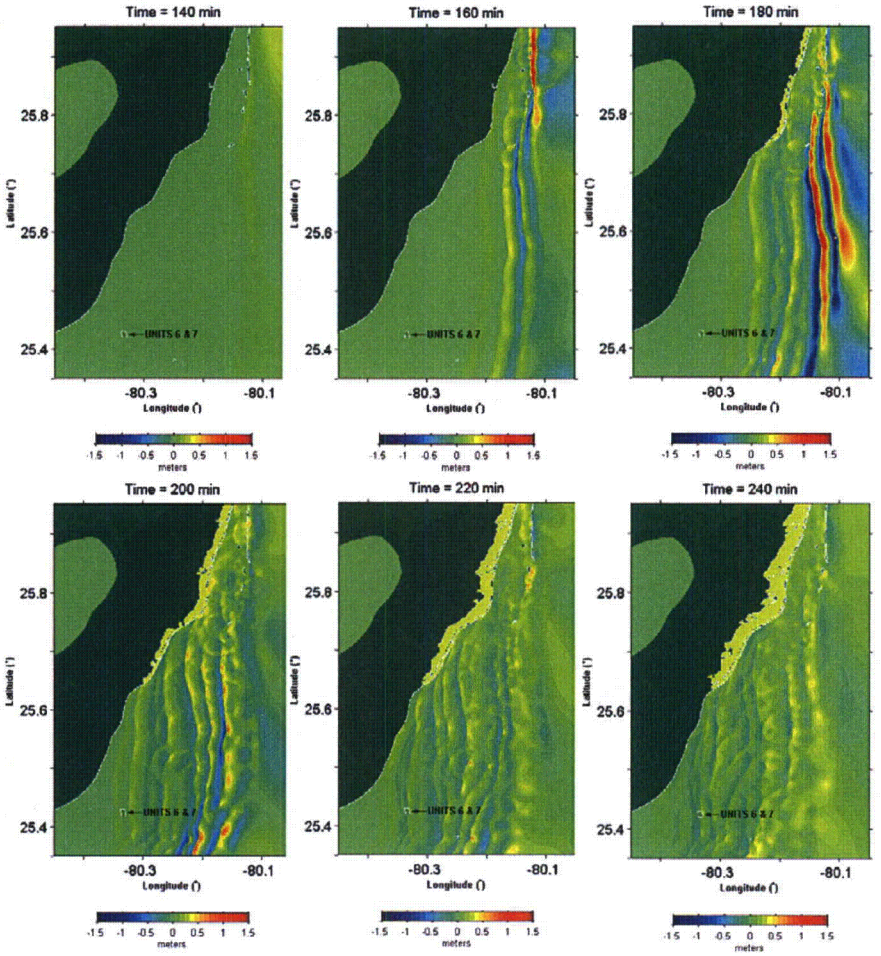

Figure 23. Simulated maximum water surface elevation during the propagation of the Cape Fear tsunami (static source) in Grid C. Colors in elevation legend represent water surface elevations relative to MLW.

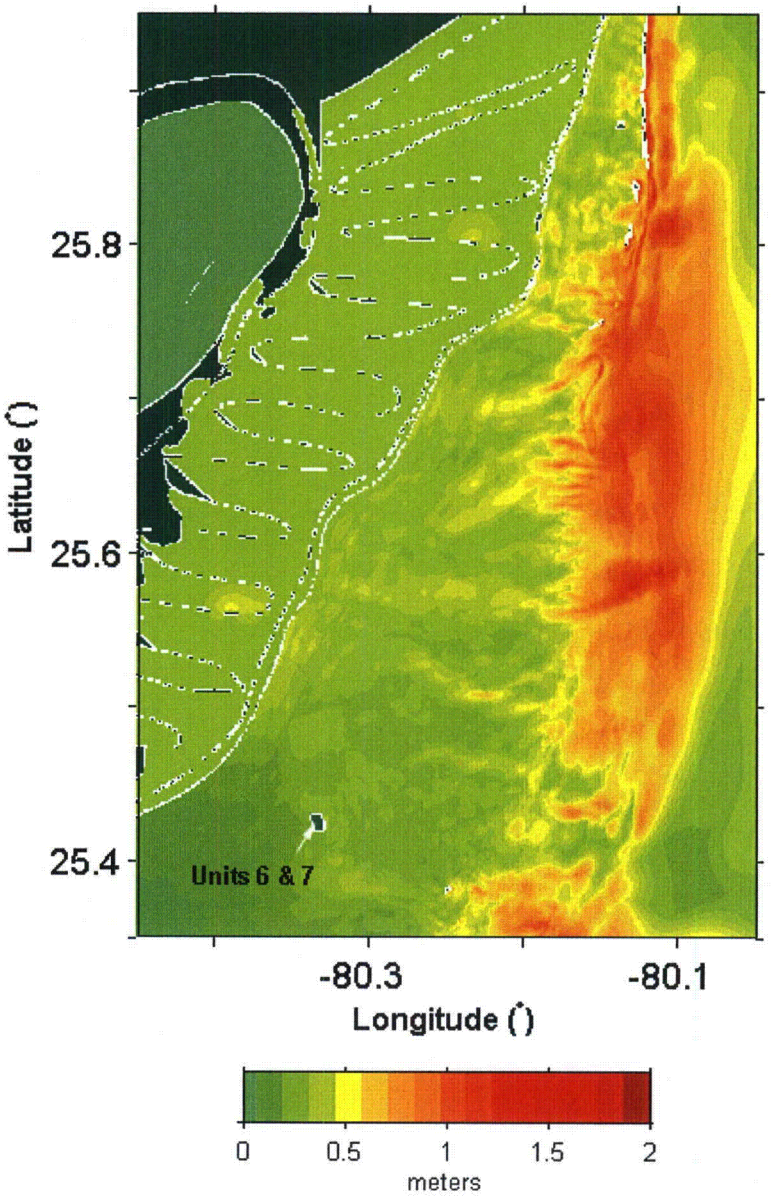

Figure 24. Simulated maximum water surface rise, relative to the initial sea water level, during the propagation of the Cape Fear tsunami (static source) in the vicinity of Units 6 & 7. Colors in elevation legend represent water surface elevations relative to MLW.

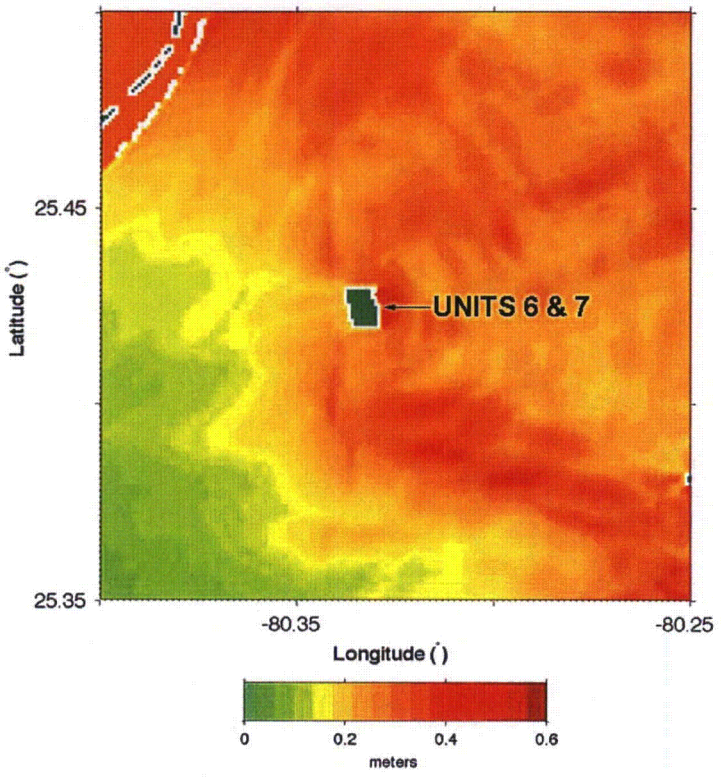

Figure 25. Water surface elevation near Units 6 & 7 as a function of time following the Cape Fear tsunami (static source). Water surface elevations in meters are relative to the initial water level.

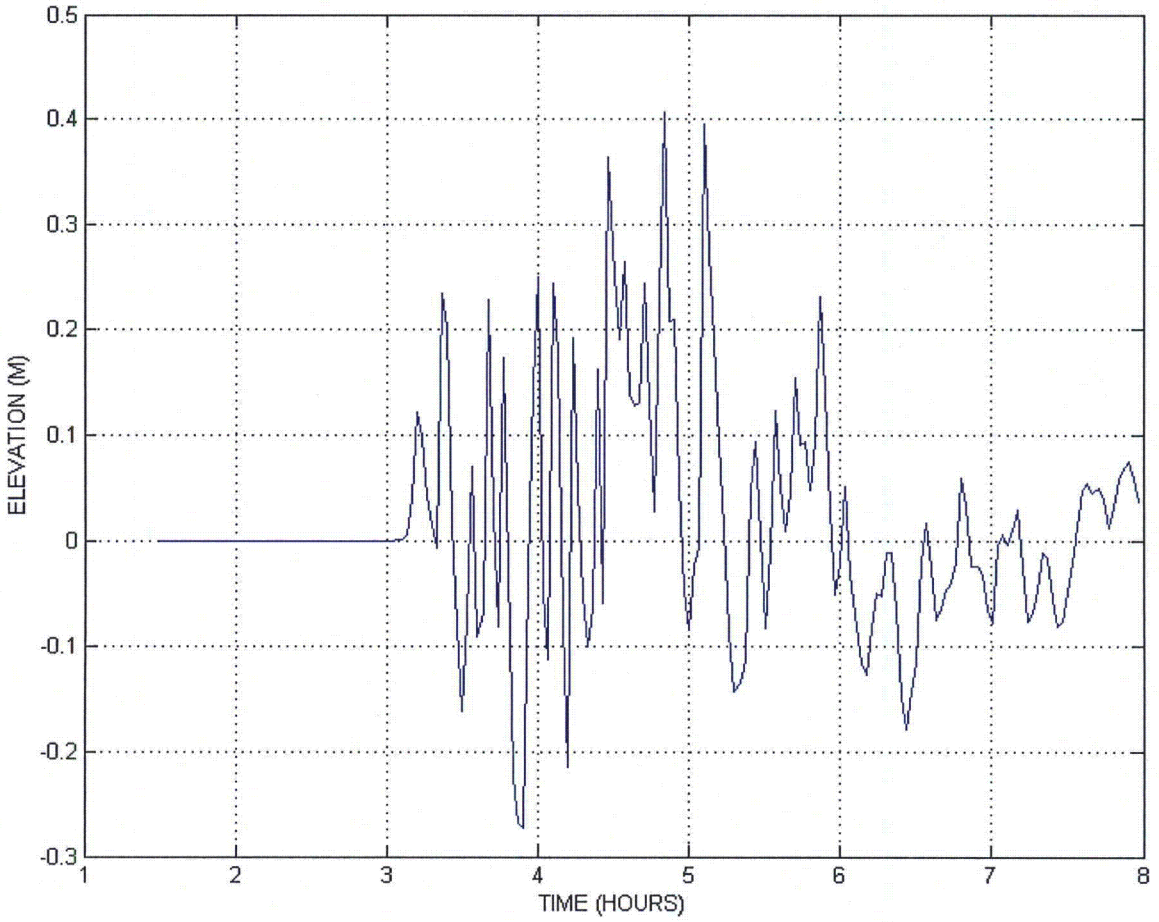

This response is PLANT SPECIFIC.

References:

1. Popenoe, P., Schmuck, E. A. and W. P. Dillon, "The Cape Fear landslide: Slope failure associated with salt diapirism and gas hydrate decomposition", in *Submarine Landslides: Selected Studies in the U.S. Exclusive Economic Zone*, Schwab, W.C., Lee, H. J. and D. C. Twichell (eds.), U.S. Geological Survey Bulletin 2002, pp. 40–53, 1993.
2. Popenoe, P., and Dillon, W. P., "Characteristics of the continental slope and rise off North Carolina from GLORIA and seismic-reflection data: The interaction of downslope and contour current processes", in Gardner, J.V., Field, M.E., and Twichell, D.C. (eds.) *Geology of the United States' Seafloor, The View from GLORIA*, Cambridge University Press, Cambridge, United Kingdom, pp. 59-80 1996.
3. Atlantic and Gulf of Mexico Tsunami Hazard Assessment Group, *Evaluation of Tsunami Sources with the Potential to Impact the U.S. Atlantic and Gulf Coasts*, An Updated Report to the Nuclear Regulatory Commission, prepared by the Atlantic and Gulf of Mexico Tsunami Hazard Assessment Group, Revision: August 22, 2008.
4. Paull, C.K., Matsumoto, R., Wallace, P.J., et al., "Chapter 1: Introduction", *Proceedings of the Ocean Drilling Program, Initial Reports*, Vol. 164, pp. 5-12 1996.
5. Hornbach, M. J., Lavier, L. L. and Ruppel, C. D., "Triggering mechanism and tsunamigenic potential of the Cape Fear Slide complex", U. S. Atlantic margin, *Geology, Geophysics, Geosystems*, Vol. 8, no. 12, pp. 1-16, 2007.
6. Paull, C. K, Buelow, W.J., Ussler III, W., and Borowski, W.S., "Increased continental-margin slumping frequency during sea level lowstands above gas hydrate bearing-sediments", *Geology*, Vol. 24, no. 2, pp. 143-146, 1996.
7. Lee, H.J., "Timing of occurrence of large submarine landslides on the Atlantic Ocean margin", *Marine Geology*, Vol. 264, no. 1-2, pp. 53-64, 2009.
8. Rodriguez, N.M. and Paull, C.K., "Chapter 32. Data Report: ^{14}C Dating of Sediment of the Uppermost Cape Fear Slide Plain: Constraints on the Timing of this Massive Submarine Landslide", in *Proceedings of the Ocean Drilling Program, Scientific Results*, Paull, C. K., Matsumoto, R., Wallace, P. J., and W. P. Dillon (eds.), Vol. 164., pp. 325-327, 2000.
9. Owen, M., Day, S., and M. Maslin, "Late Pleistocene submarine mass movements: occurrence and causes", *Quaternary Science Reviews*, Vol. 26, no. 7-8, pp. 958-978, 2007.
10. Tappin, D. R., "Submarine mass failures as tsunami sources: their climate control", *Philosophical Transactions of the Royal Society A.*, vol. 368, pp. 2417-2434, 2010.

11. Twichell, D. C., Chaytor, J. D., ten Brink, U. and B. Buckowski, "Morphology of late Quaternary submarine landslides along the U.S. Atlantic continental margin", *Marine Geology*, vol. 264, no. 1-2, pp. 4-15, 2009.

12. Enet, F. and Grilli, S. T., "Experimental study of tsunami generation by three-dimensional rigid underwater landslides", *Journal of Waterway, Port, Coastal and Ocean Engineering*, Vol. 133, no. 6, pp. 442-454, 2007.

13. Carpenter, G., "Coincident sediment slump/clathrate complexes on the U.S. Atlantic continental slope", *Geo-Marine Letters*, Vol. 1, no. 1, pp. 29–32, 1981.

14. Grilli, S. T. and P. Watts, "Tsunami generation by submarine mass failure, Part I: modeling, experimental validation, and sensitivity analyses", *Journal of Waterway, Port, Coastal, and Ocean Engineering*, Vol. 131, no. 6, pp. 283-297, 2005.

15. ten Brink, U., Twichell, D., Lynett, P., Geist, E., Chaytor, J., Lee, H., Buczkowski, B. and C. Flores, *Regional assessment of tsunami potential in the Gulf of Mexico: U.S. Geological Survey Administrative Report*, Report to the National Tsunami Hazard Mitigation Program, Revision: September 2, 2009.

16. Shi, F., Kirby, J. T. and B. Tehranirad, *Tsunami benchmark results for spherical coordinate version of FUNWAVE-TVD (Version 1.1)*, Research Report No. CACR-12-02, Center for Applied Coastal Research, University of Delaware, Newark, 2012.

17. Tehranirad, B., Shi, F., Kirby, J. T., Harris, J. C. and S. T. Grilli, *Tsunami benchmark results for fully nonlinear Boussinesq wave model FUNWAVE-TVD, Version 1.0*, Research Report No. CACR-11-02, Center for Applied Coastal Research, University of Delaware, Newark, 2011.

18. Shi, F., Kirby, J. T., Tehranirad, B., Harris, J. C. and S. T. Grilli, *FUNWAVE-TVD Version 1.0, Fully nonlinear Boussinesq wave model with TVD solver, Documentation and User's Manual*, Research Report No. CACR-11-04, Center for Applied Coastal Research, University of Delaware, Newark, 2011.

19. Synolakis, C. E., Bernard, E. N., Titov, V. V., Kanoglu, U. and Gonzalez, F. I., *Standards, criteria, and procedures for NOAA evaluation of tsunami numerical models*, NOAA Technical Memorandum OAR PMEL-135, Pacific Marine Environmental Laboratory, Seattle, 2007.

20. Ma, G., Shi, F. and Kirby, J. T., "Shock-capturing non-hydrostatic model for fully dispersive surface wave processes", *Ocean Modelling*, Vol. 43-44, 22-35, 2011.

21. Liu, P. L-.F., Lynett, P. and C. Synolakis, "Analytical solutions for forced long waves on a sloping beach", *J. Fluid Mech.* 478: 101-109, 2003.

22. Amante, C. and B. W. Eakins, *ETOPO1 1 arc-minute Global Relief Model: Procedures, data sources and analysis*, NOAA Technical Memorandum NESDIS NGDC-24, 19 pp., 2009

23. National Oceanic and Atmospheric Administration (NOAA), *NGDC 3 Arc-Second Coastal Relief Model Development*, available at :http://www.ngdc.noaa.gov/mgg/coastal/model.html accessed on April 20, 2012.

ASSOCIATED COLA REVISIONS:

The following changes in FSAR Subsection 2.4.6.1.1 will be included in a future revision of the COLA.

2.4.6.1.1 Submarine Landslides along the U.S. Atlantic Margin

Submarine landslide zones along the U.S. Atlantic margin are concentrated along the New England and Long Island, New York sections of the margin, outward of major ancient rivers in the mid-Atlantic region, and in the salt dome province offshore of North and South Carolinas, as shown in Figure 2.4.6-201 (Reference 202). Although submarine landslides along the U.S. Atlantic margin, from Georges Bank offshore of the New England coast to Blake Spur south of the Carolina Trough, have the potential to cause devastating tsunamis locally, the presence of a wide continental shelf is expected to reduce their impact at the shoreline near the landslides (Reference 202).

AGMTHAG mapped a total of 48 landslide affected areas based on data compiled from bathymetry, GLORIA (Geological Long-Range Inclined Asdic) sidescan sonar imagery, seismic reflection profiles, and sediment core data (Reference 202). The general characteristics of the mapped landslides are summarized in Table 2.4.6-201. The distribution of landslide locations identified along the U.S. Atlantic margin from the Georges Bank to the Carolina Trough is shown in Figure 2.4.6-202. The largest submarine landslide area near Units 6 & 7 is the Cape Fear Slide ~~(CFS)~~ complex, identified in an area south of Cape Hatteras, off the Carolina Trough. ~~The largest landslide in this area exceeds 15,241 square kilometers (5885 square miles) with a volume in excess of 150 cubic kilometers (36 cubic miles). Tectonic activities of the salt domes have been suggested as the triggering mechanism for the landslides in this area along with suggestions that decomposition of gas hydrates due to sea level change and small shallow earthquakes may also have contributed to the formation of these landslides (Reference 202).~~ **The Cape Fear Slide headwall is described as an amphitheater-shaped scarp centered on a lower slope at a depth of approximately 2300 to 2600 meters, 50 kilometers long, and approximately 120 meters high. Within the headwall's failure area, two large salt diapirs project above the sea floor. A complex of slumps extends more than 40 kilometers upslope from the major headwall scarp, and mass-movement deposits are traceable for more than 400 kilometers downslope to a water depth of over 5.4 kilometers on the Hatteras Abyssal Plain (References 202, 223, 225, 226 and 227). Longitudinal lines in the 1987 GLORIA side-scan sonar image, Figure 2.4.6-238, (reproduced from Figure 4 in Reference 225), is interpreted as evidence of mass movement. The longitudinal lines represent both debris chutes between the salt diapirs at the head of the landslide area indicated by the Label A in Figure 2.4.6-238, and debris flow paths further downslope indicated by the Label B (Reference 225). In the proximal area of the landslide, Label C in Figure 2.4.6-238, an area of irregular, hummocky topography on the sea floor provides evidence of mass movement. At the distal portion of the slide, the landslide material extends across an older slope failure, the Cape Lookout Slide (Reference 225).**

Multibeam swath bathymetric data from the SeaBeam 2100/12 system and single channel Chirp data using a Knudsen 320B/R echosounder acquired in 2007 (Reference 223), provide the basis for a new interpretation of the Cape Fear slide. The multibeam bathymetric images combined with the Chirp data revealed at least five major escarpments (labeled S1 through S5 in Figure 2 of Reference 223). The S1 scarp is the westward and shallowest of the scarps, at approximately 890 meters below sea level, and with a crown-shaped headwall that extends 40 kilometers downslope of both sides of the slide scar. The S1 scarp crosscuts the S4 and S5 scarps and extends upslope of the main headwall (S4 and S5 headwalls). The S2 and S3 scarps are located within the S1 debris field. The S2 scarp is approximately 20 kilometers long and approximately three kilometers wide chute that abruptly widens downslope. The approximate headwall height for the S2 scarp is at least 30 meters. The S3 scarp is associated with the smallest disrupted area and has a height of at least 20 meters above the rupture surface. The main headwall scarp, S4, is likely the largest slide in the complex with an approximately 120-meter high headwall that extends over approximately 50 kilometers. The S5 scarp intersects the northern flank of the S4 scarp and is a secondary slide. It extends approximately 10 kilometers north of the S4 slide and has a headwall height of approximately 30 meters. In addition to collecting data on the S1 through S5 scarps, the bathymetric data showed a north-south linear depression running subparallel to the continental slope break at the extreme southern end of the S4 escarpment. The Chirp data suggests, "this ~40 kilometers long feature represents the scarp of a previously unrecognized, seafloor breaking normal fault" (Reference 223).

Based on radiocarbon (C-14) analyses of core samples from within 50 kilometers of the slide's headwall, the age of the slide is estimated as between 9 to 14.5 thousands of years (References 228 and 229). However, an unconformity occurs between 0.5 and 2 meters depths within the Cape Fear Slide complex. The ages of the samples collected from the cores below the unconformity are older than 29 thousands of years. An interpretation of these data indicated a hiatus on the sole of the slide that separated the sediments that are younger than 14.5 thousands of years from those that are older than 29 thousands of years and that the slide was active during that time (Reference 228). This period of slide activity most likely occurred at the transition between the end of the last glaciation (Wisconsinan Stage) and the present interglacial age. This age bracket appears to be associated with the Pleistocene sea level lowstand between approximately 12,000 and 28,000 years during the last glacial maximum (References 202, 223, 227, 228, 229, 230, 231 and 232). The possible triggering mechanisms for the slide activity are salt movement, driven by sediment loading, with salt diapirism causing over steepening of the seabed slope followed by failure and potential sediment instability due to gas hydrate decomposition (References 202, 223, 230, 231 and 232).

Units 6 & 7 are located approximately 400 miles (640 kilometers) southwest of Blake Spur with a wide and shallow continental slope and shelf in between (Figure 2.4.6-201). Details of the Atlantic continental shelf near the site are described in Subsection 2.5.1.1.1.1. Additionally, the landslide zones are oriented in a manner that Units 6 & 7 would be away from the main axis of submarine landslide-generated tsunamis. The impact of any submarine landslide-generated tsunami on the continental slope and shelf north of Blake Spur would be considerably reduced before reaching Units 6 & 7. For example, Hornbach

et al. (Reference 223) simulated a tsunami generated by the largest landslide from the **Cape Fear Slide** ~~CFS~~ complex. The model results include contours of tsunami amplitudes 30 minutes after initiation of the landslide (see Figure 2.4.6-227). The major tsunami waves propagate along the axis of the landslide, both toward the coast and seaward. Geometrical spreading of the tsunami wave is prominent along the direction perpendicular to the axis of slide and toward the Straits of Florida. Based on the model results, the tsunami wave amplitude 30 minutes after slide initiation and about 200 kilometers (124 miles) along the Units 6 & 7 direction is approximately 1.5 meters (4.9 feet). In contrast, the tsunami amplitude off Miami, Florida, at a water depth of 783 meters (2569 feet) for the 1755 Lisbon Earthquake tsunami (which corresponds to the PMT) is 2.0 meters (6.6 feet) (Reference 209). The distance between the **Cape Fear Slide** ~~CFS~~ complex and the off-Miami site at a water depth of 783 meters (2569 feet) is more than 800 kilometers (497 miles). Therefore, the tsunami maximum water level at the Units 6 & 7 site due to the **Cape Fear Slide** ~~CFS~~ complex would be lower than that from the 1755 Lisbon Earthquake tsunami.

To provide additional support to the conclusion based on the results of Hornbach et al (Reference 223) and to assess independently how a tsunami generated by a submarine slope failure at Cape Fear would affect PMT water levels at the Units 6 & 7 site, numerical models were used to estimate the wave that would be generated by such a failure and simulate its propagation towards the site, as described in Subsection 2.4.6.4.2.

Twichell et al. studied submarine erosion and characterized morphologic provinces for the Blake Escarpment (Figure 2.4.6-203) northeast of Units 6 & 7 (Reference 203). The Blake Escarpment, extending approximately 450 kilometers (280 miles) to the south from Blake Spur, is one of the largest cliffs in the ocean with a relief of about 4000 meters (13,120 feet) (Reference 203). Near the southern edge of the escarpment, it crosses with the Jacksonville fracture zone, which underlies the Blake plateau at the location of Abaco Canyon. The escarpment was isolated from the continent-derived sediments since late Cretaceous, first by the currents in the Suwannee Straits and later by the Gulf Stream, and erosion of the escarpment is evident over the period (Reference 203).

The following changes in FSAR Subsection 2.4.6.4 will be included in a future revision of the COLA.

2.4.6.4 Tsunami Analysis

The maximum tsunami water level at Units 6 & 7 is obtained for the postulated PMT generated by earthquake in the Azores-Gibraltar fracture zone. Tsunami propagation and the effects of near shore bathymetric variation at the Florida Atlantic coast are simulated in a two-dimensional computer model, the development of which is summarized in the following subsections. Detailed water level records near Units 6 & 7 are not available for tsunamis generated by past earthquakes in the Azores-Gibraltar fracture zone or in the Caribbean subduction zone for the listed earthquake magnitudes. In order to establish the model boundary condition, the resulting water levels in deep waters in the computer simulations by Mader (Reference 202) and Knight (Reference 211) for tsunamis generated from the Azores-Gibraltar and Caribbean sources are used as guidance for the PMT model. The PMT simulation for Units 6 & 7 uses the computer code Delft3D-Flow, which is a multi-dimensional modeling system that is capable of simulating the hydrodynamics and transport

processes for fluvial, estuarine, and coastal environments (Reference 219). **The analysis of the postulated PMT is described in Subsection 2.4.6.4.1.**

In addition the generation and propagation of a tsunami caused by the Cape Fear slide was simulated to examine the water levels it produces at the site and to confirm that they are smaller than those produced by the postulated PMT. The simulation of the Cape Fear tsunami for Units 6 & 7 uses the model FUNWAVE-TVD, which solves the solved the spherical-polar form of the weakly-nonlinear, weakly-dispersive Boussinesq equations in spherical coordinates (Reference 234). The analysis of the Cape Fear tsunami is described in the Subsection following the analysis of the PMT.

2.4.6.4.1 Analysis of the PMT (Azores-Gibraltar fracture zone earthquake tsunami)

The following FSAR subsection numbers will be revised in a future COLA revision as shown below.

2.4.6.4.**1.**1 Numerical Modeling Approach and Conceptualization

2.4.6.4.**1.**2 Model Setup

2.4.6.4.**1.**3 Selection and Validation of Open Boundary Condition

2.4.6.4.**1.**4 Sensitivity of Model Parameters and Conditions

2.4.6.4.**1.**5 Model Simulation Results

The following Subsection will be added to after FSAR Subsection 2.4.6.4.1.5 in a future revision of the COLA as shown below.

2.4.6.4.2 Analysis of the Cape Fear Tsunami

2.4.6.4.2.1 Representation of the Cape Fear Slide in the Model

The maximum potential slide at Cape Fear was schematized for modeling purposes as having a Gaussian shape with an elliptical footing that extends from the uppermost head scarp to the salt diapirs in the downslope region. This shape was chosen because a Gaussian shape has been used for several investigations and studies of landslide tsunamis, including benchmark cases (References 237, 242, 243). Grilli and Watts (Reference 237) state that a Gaussian shape is a more realistic representation of a submarine mass failure than other arbitrary fixed shapes. Enet & Grilli (Reference 235) used a Gaussian shape in the experiments that provide the basis for the validation of the model used to simulate the generation of a wave by a submarine slide (Reference 235). The Gaussian shape of the slide was approximated in the numerical model by truncated hyperbolic secant squared functions (Reference 235). The center of the elliptical base of the slide was initially located near the S1 headwall in Figure 2 of Reference 223, at 33.14° N, 76.29° W, which places the uppermost end of the slide area at a depth of approximately 710 meters.

The length (minor axis of the elliptical base) of the slide is 38 kilometers, based on the distance from the upper scarp (described as S1 in Reference 223 and as the upper headwall scarp in Reference 225) to the salt diapirs downslope shown in Figure 2 of Reference 223. This length represents a conservative upper bound for the length

of a potential slide. The width (major axis of the elliptical base) of the slide was assumed to be 50 kilometers taken conservatively from the width of the largest scarp S4 (the main scarp). The use of 50 kilometers as the width (reported as 10 kilometers in Reference 223) of the slide is conservative as it is five times the width of the upper scarp at the centroid of the postulated slide.

The maximum thickness of the postulated slide was taken as approximately 120 meters. This thickness is equal to the maximum height of the main scarp of the Cape Fear slide, S4, located at 2300 meters depth, and is larger than the thicknesses of all the other scarps. For instance, the height of the uppermost scarp at 890 meters depth is much smaller, at about 20 meters (Reference 236). Using a thickness of 120 meters is therefore a conservative assumption because the centroid of the postulated slide for the tsunami simulations is placed near the uppermost scarp, S1, at much smaller depth than the lower scarp of the Cape Fear slide. The assumed dimensions and shape of the postulated slide give an area of 1492 km^2 for the base of the slide and a total volume of 68 km^3.

The bottom slope used was 3.09 degrees, based on a measured depth difference of 1350 meters over a distance of 25 kilometers in the area of the downslope movement of the slide. The distance of 25 kilometers is based on the presence of a slope break in the Cape Fear profile at about 25 kilometers from the initial location of the centroid, after which the slope decreases by approximately one-half. The direction of the downslope movement of the slide forms a 10 degree angle clockwise with the West-East direction. This direction is based on the delineation and orientation of the Cape Fear slide from the GLORIA mapping data.

The initial acceleration of the slide, 0.529 m/s^2, was estimated directly from the bed slope. Using Equation (10) in Reference 235, the terminal velocity of the slide was estimated to be 138 m/s. As stated earlier, this estimate was obtained using a specific gravity for the slide equal to 2 (Reference 223), and a bed slope of 3.09 degrees, and a length of 38 kilometers. The global drag coefficient was set equal to 1 (Reference 237), which is conservative. Based on its initial acceleration, the slide reaches its terminal velocity within 260 seconds.

2.4.6.4.2.2 Initial Wave Generated by the Cape Fear Slide

Two alternative approaches were used for the generation of the initial wave in the tsunami simulations. The two approaches are referred to as the dynamic source approach and the static source approach. Two source approaches are used as the velocity components from the dynamic source can differ significantly from the static source with respect to the total slide energy.

The dynamic source approach defined the initial condition for the tsunami propagation simulations in terms of both the water surface displacement and the depth-averaged horizontal velocity fields. This source was computed from the slide geometry and its movement using the computer model NHWAVE (Non-Hydrostatic Wave), Version 1.1 (Reference 238). NHWAVE solves the fully non-hydrostatic Navier-Stokes equations in the sigma coordinate system. The model assumes a single-valued water surface and represents turbulent stresses in terms of an eddy viscosity closure scheme. Turbulent stresses are not modeled, and thus the model is

basically solving the Euler equations for incompressible flow with a moving surface and bottom.

Input to NHWAVE includes the bathymetric grid, the slide dimensions, the initial slide position and orientation, and the terminal velocity. The modeled domain was set up so that the landslide event was centrally located and the generated motion did not reach the lateral boundaries during the simulated time. Bathymetric data for the model domain of NHWAVE and the three nested grids of FUNWAVE-TVD used in the simulations were obtained from the National Geophysical Data Center (NGDC) ETOPO 1 (Reference 244) and the Coastal Relief Model (CRM) (Reference 245) data sets. Results from the NHWAVE model output at 500 seconds were saved and used as initial conditions in the tsunami propagation model FUNWAVE-TVD. The reason for selecting the NHWAVE solution at 500 seconds as input to the tsunami propagation model, was that at that time the maximum wave height is about equal to the maximum thickness of the slide (120 meters). After 500 seconds, the NHWAVE model produces wave heights greater than the maximum thickness of the slide, which would be overly conservative.

At 500 seconds, the slide volume moves downslope 64.6 kilometers, i.e., a distance equal to 1.7 times the length of the minor axis of the elliptical base of the slide, which is aligned with the direction of downslope movement (38 kilometers). The present approach neglects the spreading and flattening of the sliding mass during the slide process. This assumption results in a higher and narrower initial elevation hump at the final slide location than what would have occurred if the slide were allowed to deform. The initial and final positions of the slide are displayed in Figure 2.4.6-239. The water depth at the initial location of the centroid of the slide is 1100 meters. The water depth at the final position of the centroid of the slide is 3300 meters (Figure 2.4.6-239).

The resulting water surface displacement from NHWAVE at that time (500 seconds) is shown in Figure 2.4.6-240 and Figure 2.4.6-241, which also shows the water surface profile in the direction of the slide motion simulated with NHWAVE at different times after the initiation of the slide. As shown in Figure 2.4.6-241, the maximum water surface at 500 seconds is 122 meters, and the minimum –166 meters.

The second approach to the generation of the initial condition for the tsunami propagation model used a static source based on the geometry of the initial and final positions of the slide mass. A static source is defined as an initial displacement of the water surface in the form of a depression over the initial slide location, equal in areal extent, shape and volume to the displaced material volume during the submarine slide. It was assumed that the initial slide volume described above translates downslope along its axis in the direction of the slope beyond its original footprint. A positive displacement of the water surface equal to the volume shape and size of the slide was assumed at that point, i.e., extending over an elliptical area with minor axis equal to 38 kilometers, a major axis of 50 kilometers and maximum thickness 120 meters, and a corresponding negative displacement representing the missing volume of the slide mass was added at the slide starting point. The centroid of the depression of the water surface was placed at 33.14° N, 76.29° W, same as the initial location of the centroid of the slide for the dynamic source. A water rise equal in shape and size with the depression was assumed downslope of the initial

depression and at a distance equal to translation distance of the dynamic case, i.e., over a distance of 64.6 kilometers. The maximum water surface rise is equal to 120 meters. Figure 2.4.6-242 shows the assumed initial water surface wave for the Cape Fear tsunami simulation with FUNWAVE-TVD based on a static source. Using an initial static source, it was assumed that the initial horizontal velocities were zero over the entire model domain of FUNWAVE-TVD.

2.4.6.4.2.3 Modeling of Tsunami Propagation and Inundation

The propagation, shoreline runup and inundation caused by the Cape Fear tsunami were simulated using the Boussinesq wave model FUNWAVE-TVD, developed at the University of Delaware. In its present application, FUNWAVE-TVD solved the spherical-polar form of the weakly-nonlinear, weakly-dispersive Boussinesq equations described in Reference 234. Reference 240 describes the operation of both Cartesian and spherical-polar versions of the code. The model incorporates bottom friction and subgrid lateral turbulent mixing effects.

The Cartesian coordinate version of FUNWAVE-TVD, described in References 240 and 241, has been validated using several PMEL-135 benchmarks (Reference 242), which are the presently accepted benchmarking standards adopted by the National Tsunami Hazard Mitigation Program (NTHMP) for judging model acceptance for use in development of coastal inundation maps and evacuation plans. Benchmark tests for the Cartesian version of FUNWAVE-TVD are described in Reference 240. Benchmark tests for the spherical version of the code are described in Reference 234.

The equations solved by FUNWAVE-TVD consist of a depth-integrated volume conservation equation together with depth-integrated horizontal momentum equations. These equations are summarized in Reference 234. For tsunami applications, FUNWAVE-TVD is run with closed boundaries and an initial hot start condition consisting of either a surface displacement alone (in the case of static initial conditions) or a surface displacement and initial velocity field (in the case of a dynamic initial condition based on the results of calculations with NHWAVE). The model is run from the initial start until past the time when significant wave activity has decayed at the target site.

In most large scale problems, FUNWAVE-TVD is run on more than one nested grid. The grid nesting scheme uses a one-way nesting technique, which passes surface elevation and velocity components calculated from a large domain to a nested small domain through ghost cells at nesting boundaries. A linear interpolation is performed between the large and the small domain at the nesting boundaries. A test of the nesting process is included in the FUNWAVE-TVD verification and validation document (Reference 234).

In the simulations of the Cape Fear tsunami, three nested grids are used, which are referred to as Grid A, Grid B and Grid C. The output from Grid A is used as input to FUNWAVE-TVD on Grid B. The same process is repeated in going from Grid B to Grid C.

The domain covered by each of these three grids is shown in Figure 2.4.6-243. All the grids are based on geographic coordinates. The coordinates of the southwest corner

of each grid, the grid spacing, and number of grid cells in each grid are given Table 2.4.6-205.

It is noted that because of the curvature of the earth, having a uniform grid size in degrees leads to variable-length (in the west-east direction) cells at different latitudes within the model domain.

There is a sponge layer along the open boundaries of the model, which was used for the definition of the boundary conditions. The thickness of the sponge layer was 200 kilometers along the eastern boundary, and 100 kilometers along the northern and southern boundaries.

The antecedent water surface level was equal to the 10 percent exceedance spring tide level, plus the initial rise and long term sea level rise, which produce an initial water level equal to 1.68 meters (5.5 feet) mean low water (MLW), or 3.6 feet (1.10 meters) NAVD 88.

2.4.6.4.2.4 Simulation Results

Two sets of simulation results for the tsunami propagation and inundation by the Cape Fear tsunami are presented. The first set of results is for the dynamic initial condition and the second set of results is for a static initial condition.

Dynamic Source Initial Condition

Figure 2.4.6-244 and Figure 2.4.6-245 show the propagation of the tsunami wave over the domain of model Grid A during the first three hours of the FUNWAVE-TVD simulation, presenting snapshots of the wave height every 20 minutes. Time zero in the FUNWAVE-TVD simulation is 500 seconds after the initiation of the slide. It should be noticed that the color scale indicating wave height differs in the different panels of these two figures. As can be seen in these figures, the highest waves travel towards the east. The wave traveling west towards the east coast of the United States is relatively smaller. Relatively high water levels are also predicted towards the southeast. This is illustrated in Figure 2.4.6-246 which shows the maximum water surface elevation within the model domain of Grid A during the simulation period. The highest water levels are within a fan-shaped zone towards the east, and over a relatively narrow zone towards the southeast. The latter seems to coincide with the relatively shallower ocean depths along Blake Ridge (Figure 2.4.6-243).

Figure 2.4.6-247 shows the propagation of the tsunami wave in Grid B, from 100 minutes in the FUNWAVE-TVD simulation, a little after the wave enters the Grid B domain, until 180 minutes after the slide. Snapshots of the wave height every 20 minutes are shown. Figure 2.4.6-248 shows the maximum water surface elevation within the model domain of Grid B during the simulation period. As can be seen in this Figure, the highest water levels occur in the northern part of Grid B, while the water levels toward the south and in the vicinity of Units 6 & 7 are much lower.

Figure 2.4.6-249 shows the propagation of the tsunami wave in Grid C, from 140 minutes until 240 minutes in the FUNWAVE-TVD simulation. Snapshots of the wave height every 20 minutes are shown. Figure 2.4.6-250 shows the maximum water level over Grid C. As can be seen in these figures, the area surrounding the site of Units 6 & 7 is inundated. However, the Units 6 & 7 site itself and other parts of the Turkey

Point station, which are elevated above the existing grade, are not inundated and remain dry. However, this is not caused by the Cape Fear tsunami. It is a consequence of the assumption regarding the initial sea water level rise which accounts for the 10 percent exceedance spring tide level, 3.6 feet mean low water (MLW), initial rise, 0.9 feet, and long term sea level rise, 1.0 foot, which produce an initial water level, i.e., prior to the arrival of the tsunami, equal to 1.68 meters (5.5 feet) (MLW), or 3.6 feet (1.10 meters) NAVD 88. This initial level is enough to inundate a large zone along the Florida coast, including the entire area around Units 6 & 7. This is made clear in Figure 2.4.6-251, which shows the water depth over the area of Grid C relative to two different levels of the water surface. The left panel shows the water depth relative to MLW. The right panel shows the water depth relative to the assumed initial water surface in the Cape Fear tsunami simulations, i.e., relative to MLW + 10 percent exceedance spring tide + initial rise + long-term sea level rise. As can be seen in the right panel of Figure 2.4.6-251, the area surrounding Units 6 & 7 is inundated even prior to the arrival of the tsunami. Again, the Units 6 & 7 site itself and other parts of the Turkey Point station, which are elevated above the existing grade, are not inundated and remain dry. Figure 2.4.6-252 shows the maximum water surface rise in the vicinity of Units 6 & 7, relative to the initial sea water level. The maximum water surface elevation is 2.32 meters MLW (7.5 feet) or 5.7 feet (1.75 meters) NAVD 88.

Figure 2.4.6-253 shows the water level near Units 6 & 7 from the dynamic source simulation as a function of time. The maximum water surface level rise caused by the Cape Fear tsunami is 0.6 meters over the initial water level, occurring a little after five hours from the initiation the Cape Fear slide, and about two hours after the arrival of the first waves caused by the Cape Fear tsunami.

<u>Static Source Initial Condition</u>

Figure 2.4.6-254 and Figure 2.4.6-255 show the propagation of the tsunami wave generated by a static source over the domain of Grid A during the first three hours of the FUNWAVE-TVD simulation, presenting snapshots of the wave height every 20 minutes. The tsunami propagation pattern is similar to that in the dynamic source simulation, but the wave heights away from the source, especially towards the east are much smaller than those for the dynamic sources shown in Figure 2.4.6-244 and Figure 2.4.6-245.

Figure 2.4.6-256 shows the maximum water surface elevation within the model domain of Grid A during the simulation period. Comparing Figure 2.4.6-256 with Figure 2.4.6-246 shows that the static source produces much smaller water surface elevations over most of the domain of Grid A, and especially to the east and southeast. An exception is the area right over the slide and its immediate vicinity to the west, where the maximum water surface levels with the static source are substantially higher than those obtained with the dynamic source. This difference could be attributed to the fact that in the case of the dynamic source the initial condition entered in FUNWAVE-TVD includes the velocities obtained with NHWAVE, while in the case of the static source the initial velocities in the vicinity of the source are zero. Assigning a velocity to the initial wave in the dynamic source case results

in a higher total energy than in the static source case where the initial velocity is assumed to be zero.

Figure 2.4.6-257 shows the propagation of the tsunami wave in Grid B, from 100 minutes in the FUNWAVE-TVD simulation, a little after the wave enters the Grid B domain, until 180 minutes after the slide. Snapshots of the wave height every 20 minutes are shown. Figure 2.4.6-258 shows the maximum water surface elevation within the model domain of Grid B during the simulation period. The predicted water surface levels in Grid B for the static source are quite similar to those for the dynamic source shown in Figure 2.4.6-247 and Figure 2.4.6-248.

Figure 2.4.6-259 shows the propagation of the tsunami wave in Grid C, from 140 minutes until 240 minutes in the FUNWAVE-TVD simulation. Snapshots of the wave height every 20 minutes are shown. Figure 2.4.6-260 shows the maximum water level over Grid C. Again the predicted water surface elevations over Grid C for the static source are quite similar to those predicted with a dynamic source, shown in Figure 2.4.6-249 and Figure 2.4.6-250.

Figure 2.4.6-261 shows the maximum water surface rise in the vicinity of Units 6 & 7, relative to the initial sea water level. The maximum water surface elevation is 2.08 meters (6.8 feet) MLW, or 5.0 feet (1.51 meters) NAVD 88.

Figure 2.4.6-262 shows the water level near Units 6 & 7 from the static source simulation as a function of time. The maximum water surface level rise caused by the Cape Fear tsunami is 0.4 meters, occurring a little after four hours from the initiation the Cape Fear slide, and about one hour after the arrival of the first waves caused by the Cape Fear tsunami. The maximum water level at Units 6 & 7 predicted with the static source (0.4 meters) is slightly lower than that predicted using a dynamic source (0.6 meters).

2.4.6.4.2.5 Comparison of the Cape Fear Tsunami with the PMT

The simulations of a tsunami generated by a conservatively large submarine mass failure on the continental margin off Cape Fear suggest that the impact of such an event on water levels near Units 6 & 7 will be smaller than that of the postulated PMT presented in Subsection 2.4.6.4.1. The maximum predicted water level due to the Cape Fear tsunami event is 2.28 meters (7.5 feet) MLW, or 5.7 feet (1.75 meters) NAVD 88, representing a rise of 0.6 meters of the initial sea water level. The assumed initial sea water level includes the 10 percent exceedance spring tide, 3.6 feet mean low water (MLW), an initial rise, 0.9 feet, plus the long-term sea level rise, 1.0 foot. This water level is much smaller than the maximum tsunami water level of 4.5 meters MSL (4.82 MLW) reported for the PMT case in Subsection 2.4.6.5.

The following references will be added to FSAR Subsection 2.4.6.8 in a future revision of the COLA.

225. Popenoe, P., Schmuck, E. A. and W. P. Dillon, "The Cape Fear landslide: Slope failure associated with salt diapirism and gas hydrate decomposition", in *Submarine Landslides: Selected Studies in the U.S. Exclusive Economic Zone*, Schwab, W.C., Lee, H. J. and D. C. Twichell (eds.), U.S. Geological Survey Bulletin 2002, pp. 40–53, 1993.

226. Popenoe, P., and Dillon, W. P., "Characteristics of the continental slope and rise off North Carolina from GLORIA and seismic-reflection data: The interaction of downslope and contour current processes", in Gardner, J.V., Field, M.E., and Twichell, D.C. (eds.) *Geology of the United States' Seafloor, The View from GLORIA*, Cambridge University Press, Cambridge, United Kingdom, pp. 59-80, 1996.

227. Paull, C.K., Matsumoto, R., Wallace, P.J., et al., "Chapter 1: Introduction", *Proceedings of the Ocean Drilling Program, Initial Reports*, Vol. 164, pp. 5-12, 1996.

228. Paull, C. K, Buelow, W.J., Ussler III, W., and Borowski, W.S., "Increased continental-margin slumping frequency during sea level lowstands above gas hydrate bearing-sediments", *Geology*, Vol. 24, no. 2, pp. 143-146, 1996.

229. Lee, H.J., "Timing of occurrence of large submarine landslides on the Atlantic Ocean margin", *Marine Geology*, Vol. 264, no. 1-2, pp. 53-64, 2009.

230. Rodriguez, N.M. and Paull, C.K., "Chapter 32. Data Report: 14C Dating of Sediment of the Uppermost Cape Fear Slide Plain: Constraints on the Timing of this Massive Submarine Landslide", in *Proceedings of the Ocean Drilling Program, Scientific Results*, Paull, C. K., Matsumoto, R., Wallace, P. J., and W. P. Dillon (eds.), Vol. 164., pp. 325-327, 2000.

231. Owen, M., Day, S., and M. Maslin, "Late Pleistocene submarine mass movements: occurrence and causes", *Quaternary Science Reviews*, Vol. 26, no. 7-8, pp. 958-978, 2007.

232. Tappin, D. R., "Submarine mass failures as tsunami sources: their climate control", *Philosophical Transactions of the Royal Society A.*, vol. 368, pp. 2417-2434, 2010.

233. Twichell, D. C., Chaytor, J. D., ten Brink, U. and B. Buckowski, "Morphology of late Quaternary submarine landslides along the U.S. Atlantic continental margin", *Marine Geology*, vol. 264, no. 1-2, pp. 4-15, 2009.

234. Shi, F., Kirby, J. T. and B. Tehranirad, *Tsunami benchmark results for spherical coordinate version of FUNWAVE-TVD (Version 1.1)*, Research Report No. CACR-12-02, Center for Applied Coastal Research, University of Delaware, Newark, 2012.

235. Enet, F. and Grilli, S. T., "Experimental study of tsunami generation by three-dimensional rigid underwater landslides", *Journal of Waterway, Port, Coastal and Ocean Engineering*, Vol. 133, no. 6, pp. 442-454, 2007.

236. Carpenter, G., "Coincident sediment slump/clathrate complexes on the U.S. Atlantic continental slope", *Geo-Marine Letters*, Vol. 1, no. 1, pp. 29–32, 1981.

237. Grilli, S. T. and P. Watts, "Tsunami generation by submarine mass failure, Part I: modeling, experimental validation, and sensitivity analyses", *Journal of Waterway, Port, Coastal, and Ocean Engineering*, Vol. 131, no. 6, pp. 283-297, 2005.

238. Ma, G., Shi, F. and Kirby, J. T., "Shock-capturing non-hydrostatic model for fully dispersive surface wave processes", *Ocean Modelling*, Vol. 43-44, 22-35, 2011.

239. ten Brink, U., Twichell, D., Lynett, P., Geist, E., Chaytor, J., Lee, H., Buczkowski, B. and C. Flores, *Regional assessment of tsunami potential in the Gulf of Mexico: U.S. Geological Survey Administrative Report*, Report to the National Tsunami Hazard Mitigation Program, Revision, September 2, 2009.

240. Tehranirad, B., Shi, F., Kirby, J. T., Harris, J. C. and S. T. Grilli, *Tsunami benchmark results for fully nonlinear Boussinesq wave model FUNWAVE-TVD, Version 1.0*, Research Report No. CACR-11-02, Center for Applied Coastal Research, University of Delaware, Newark, 2011.

241. Shi, F., Kirby, J. T., Tehranirad, B., Harris, J. C. and S. T. Grilli, *FUNWAVE-TVD Version 1.0, Fully nonlinear Boussinesq wave model with TVD solver, Documentation and User's Manual*, Research Report No. CACR-11-04, Center for Applied Coastal Research, University of Delaware, Newark, 2011.

242. Synolakis, C. E., Bernard, E. N., Titov, V. V., Kanoglu, U. and Gonzalez, F. I., *Standards, criteria, and procedures for NOAA evaluation of tsunami numerical models*, NOAA Technical Memorandum OAR PMEL-135, Pacific Marine Environmental Laboratory, Seattle, 2007.

243. Liu, P. L-.F., Lynett, P. and C. Synolakis, "Analytical solutions for forced long waves on a sloping beach", *J. Fluid Mech.* 478: 101-109, 2003.

244. Amante, C. and B. W. Eakins, *ETOPO1 1 arc-minute Global Relief Model: Procedures, data sources and analysis*, NOAA Technical Memorandum NESDIS NGDC-24, 19 pp, 2009.

245. National Oceanic and Atmospheric Administration (NOAA), *NGDC 3 Arc-Second Coastal Relief Model Development*, available at: http://www.ngdc.noaa.gov/mgg/coastal/model.html accessed on April 20, 2012.

The following table will be added to FSAR Subsection 2.4.6 in a future revision of the COLA.

Table 2.4.6-205
Nested Grids in FUNWAVE-TVD

Grid	Coordinates of SW Corner		Grid Spacing ($\Delta x = \Delta y$)	Number of Grid Cells
	x	y		
	degrees	degrees	seconds	cells
A	-82.0	23.0	60	780 x 900
B	-80.75	23.0	15	480 x 1260
C	-80.517	25.322	3	592 x 768

The caption for FSAR Figure 2.4.6-227 will be revised as shown below in a future revision of the COLA.

Figure 2.4.6-227. Tsunami Wave Amplitude Results for 5, 15, and 30 Min. After Slide Initiation of the Largest Landslide Within the ~~CFS~~ **Cape Fear Slide** Complex

The following figures (Figures 2.4.6-238 through 2.4.6-262) will be added to FSAR Subsection 2.4.6 in a future revision of the COLA.

Figure 2.4.6-238. GLORIA side-scan sonar image of the Cape Fear Slide

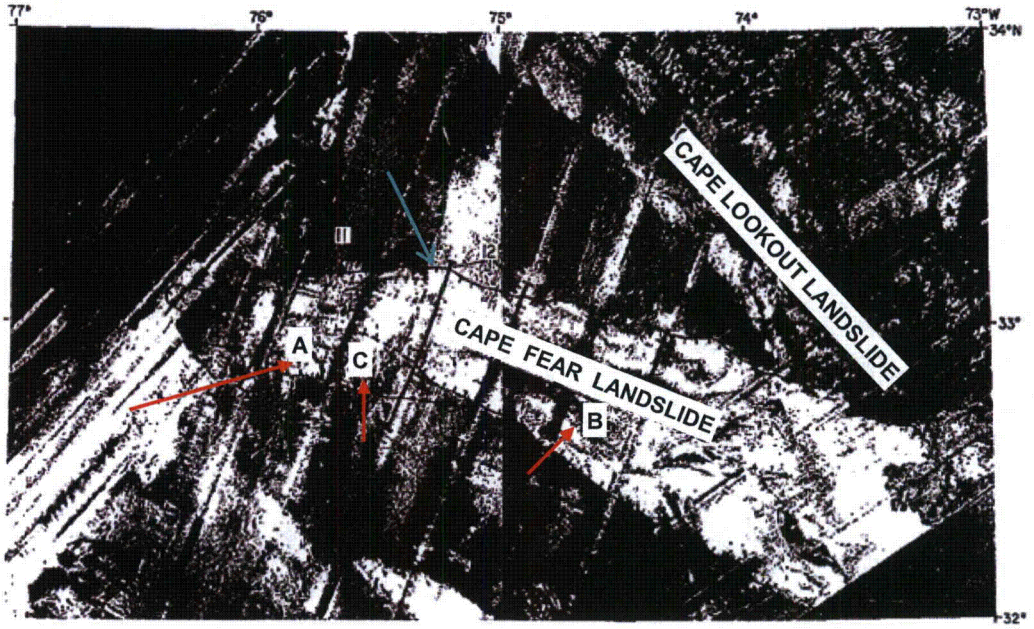

Source: Reference 225

Note: Hachures pointing downslope represents scarps. The lighter acoustic return seen in the image represent mass movement deposits and the dark return are the undisturbed sedimentary deposits. The location (A) is the longitudinal lines representing both debris chutes between the salt diapirs at the head of the landslide area, and flow paths of debris further down slope, which is shown with location (B). Location (C) is an area of irregular, hummocky sea floor that has been crumpled and buckled by mass movement near the head of the slide. The blue arrow indicates the northern limit of the Cape Fear landslide.

Figure 2.4.6-239. Location and lateral extent of the postulated submarine mass failure for the Cape Fear simulations and local bathymetry. Bathymetry contours indicate water depths (MSL).

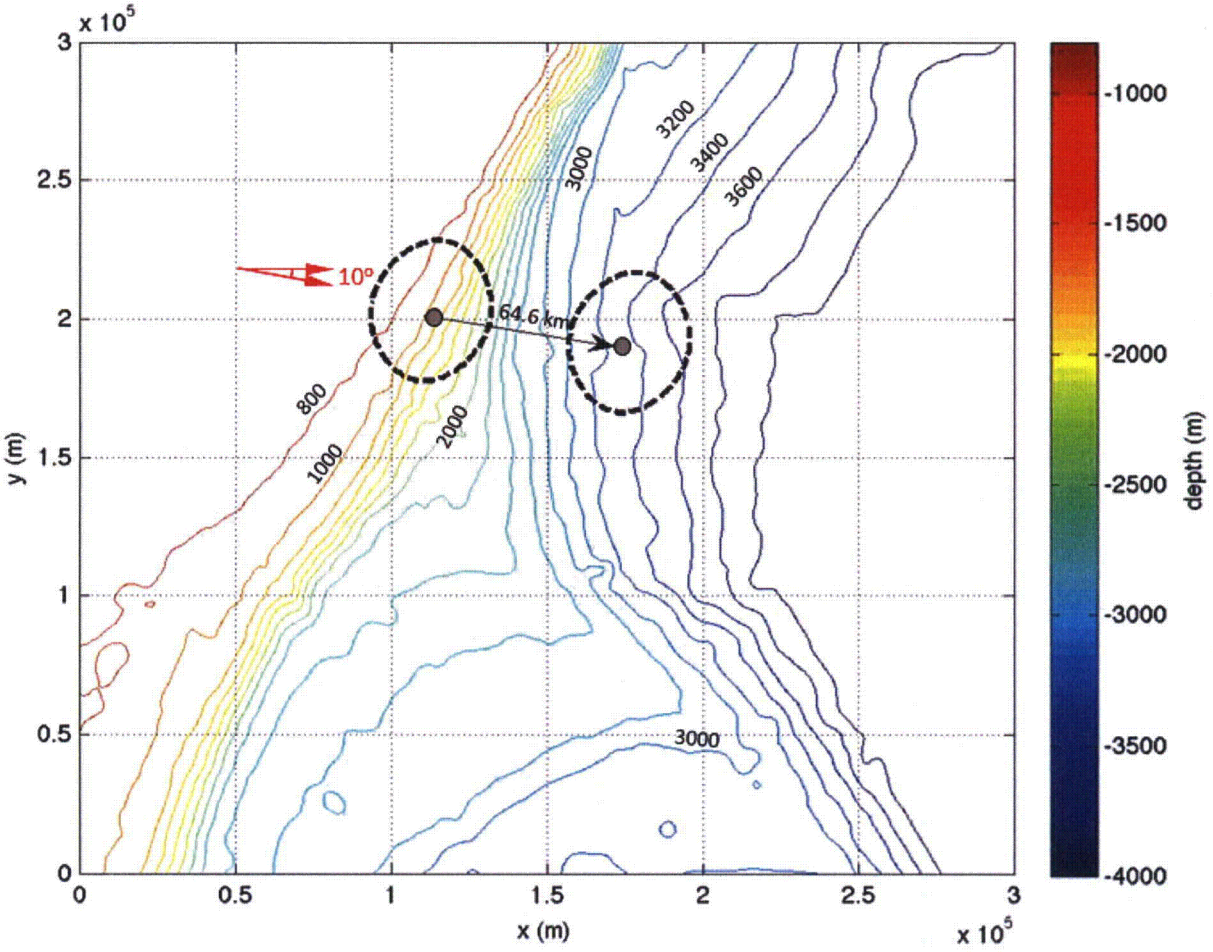

Figure 2.4.6-240. Initial wave generated by NHWAVE (dynamic source) for the Cape Fear submarine failure shown in Figure 2.4.6-239. Colors in elevation legend indicate water surface elevation (MSL) in meters. Bathymetry contours indicate water depths (m MSL).

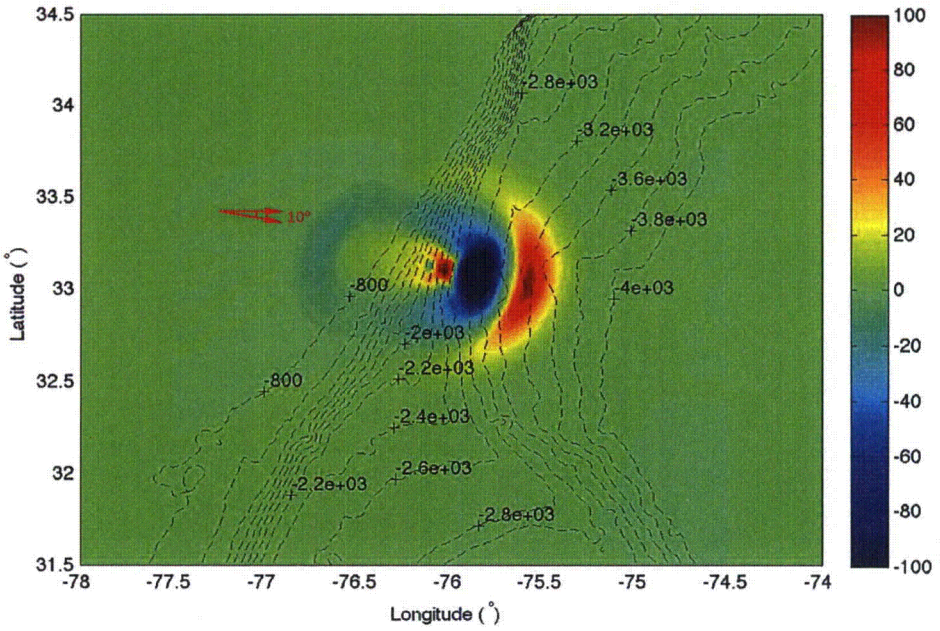

Figure 2.4.6-241. Water surface profile in the direction of the slide motion at different times after the initiation of the slide (upper panel) and ocean floor profile (lower panel). Water surface elevations (upper panel) and water depths (lower panel) are relative to MSL.

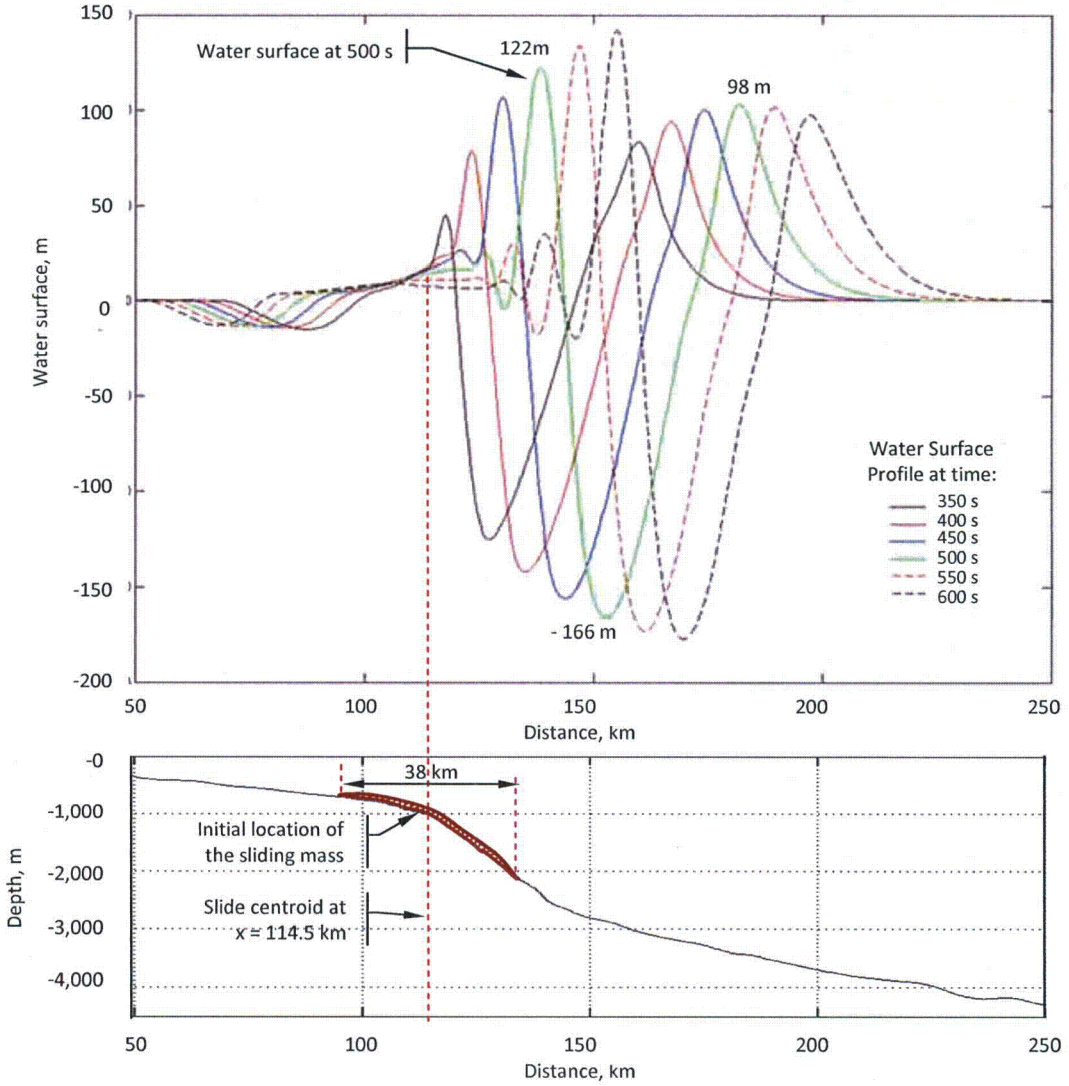

Figure 2.4.6-242. Initial wave for a static source representation of the Cape Fear submarine failure shown in Figure 2.6.4-239. Colors in elevation legend indicate water surface elevation (MSL) in meters. Bathymetry contours indicate water depths (MSL).

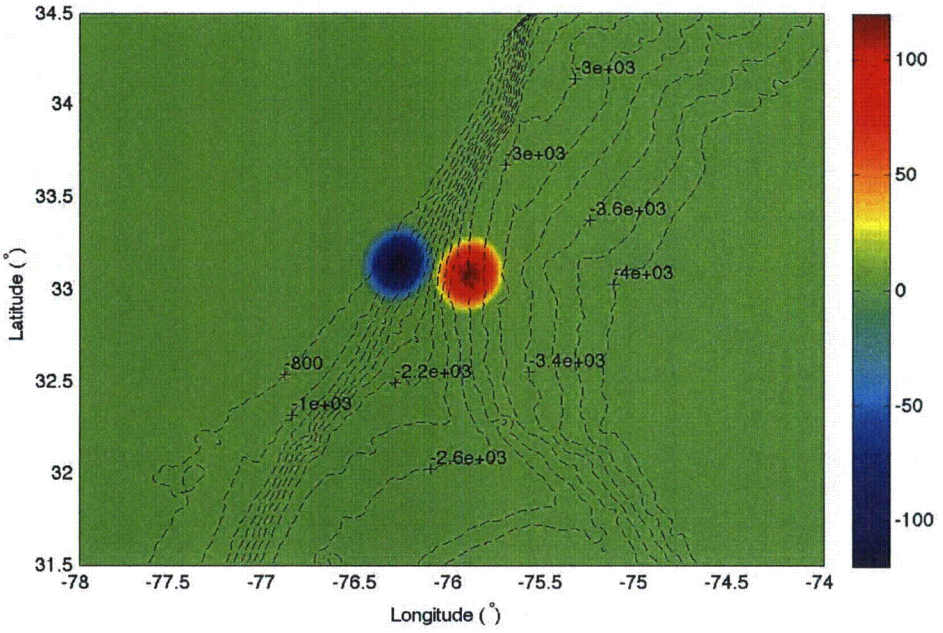

Figure 2.4.6-243. Model domain and bathymetry in the three nested grids used in the FUNWAVE-TVD simulations. Colors in elevation legend represent water surface elevations relative to MSL for ETOPO1 data and MLW for Coastal Relief Model data.

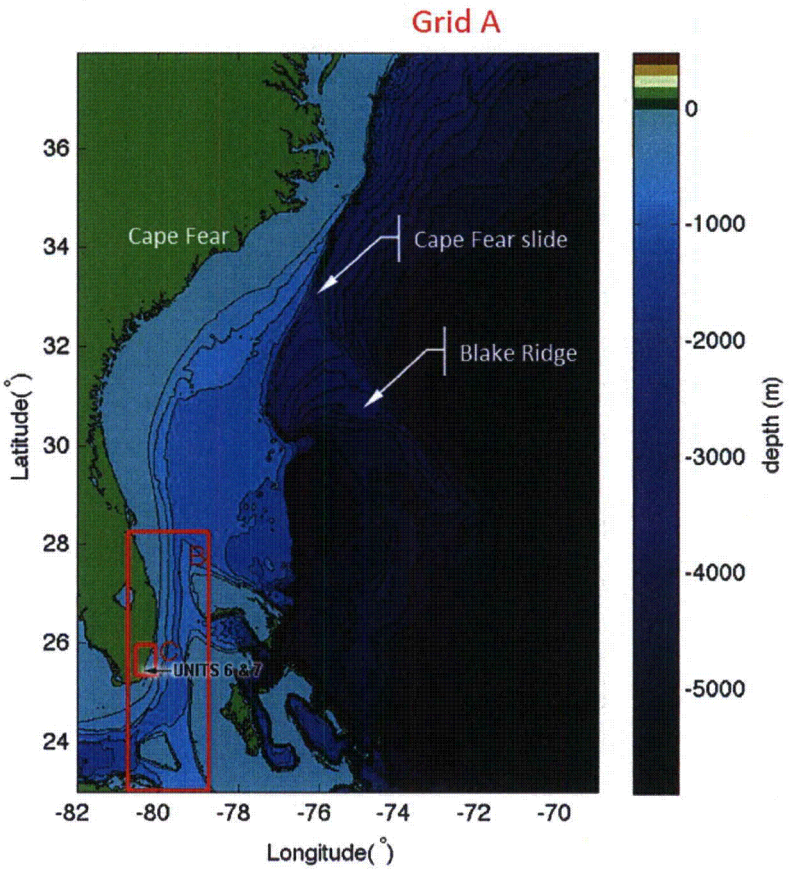

Figure 2.4.6-244. Simulated propagation of the Cape Fear tsunami (dynamic source) in Grid A at 0, 20, 40, 60, 80 and 100 minutes after the submarine failure. Colors in elevation legend represent water surface elevations relative to MSL for ETOPO1 data and MLW for Coastal Relief Model data.

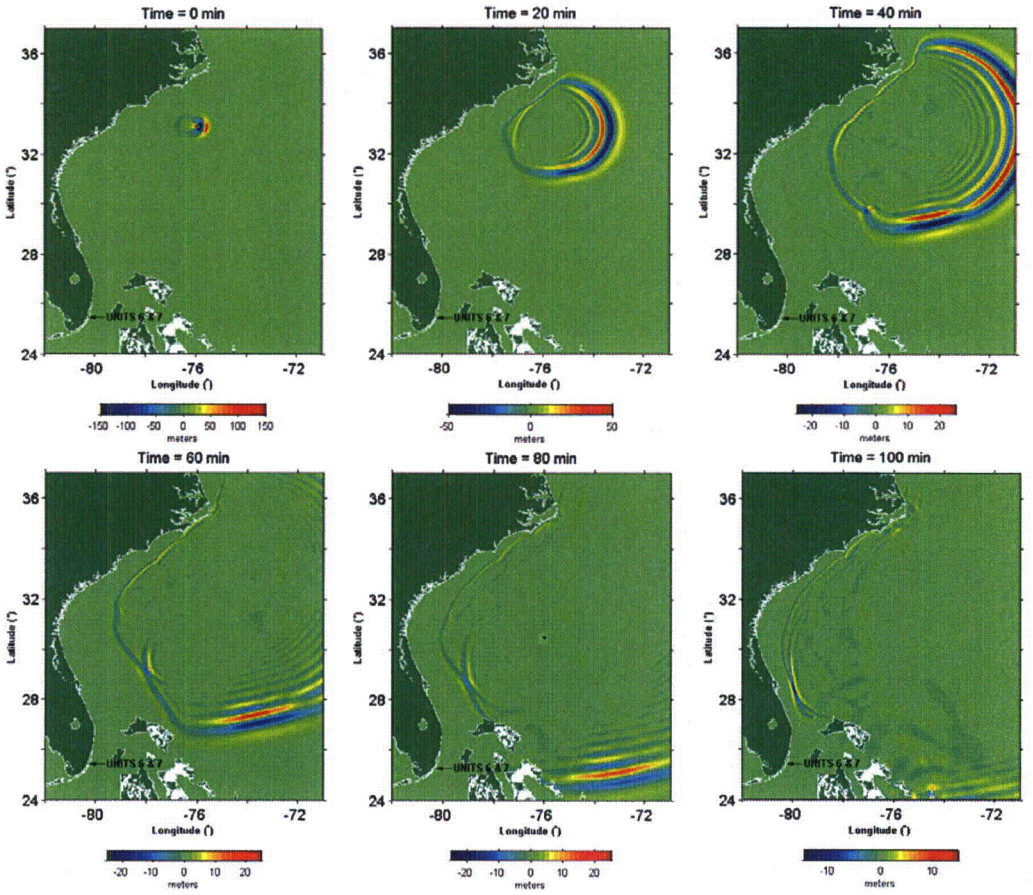

Figure 2.4.6-245. Simulated propagation of the Cape Fear tsunami (dynamic source) in Grid A at 120, 140, 160, and 180 minutes after the submarine failure. Colors in elevation legend represent water surface elevations relative to MSL for ETOPO1 data and MLW for Coastal Relief Model data.

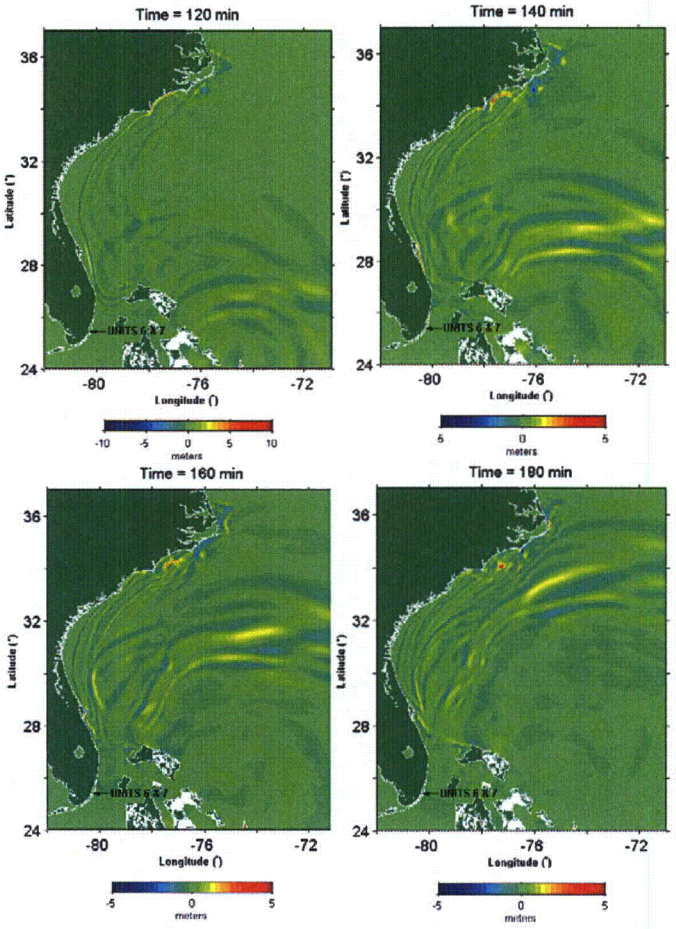

Figure 2.4.6-246. Simulated maximum water surface elevation during the propagation of the Cape Fear tsunami (dynamic source) in Grid A. Colors in elevation legend represent water surface elevations relative to MSL for ETOPO1 data and MLW for Coastal Relief Model data.

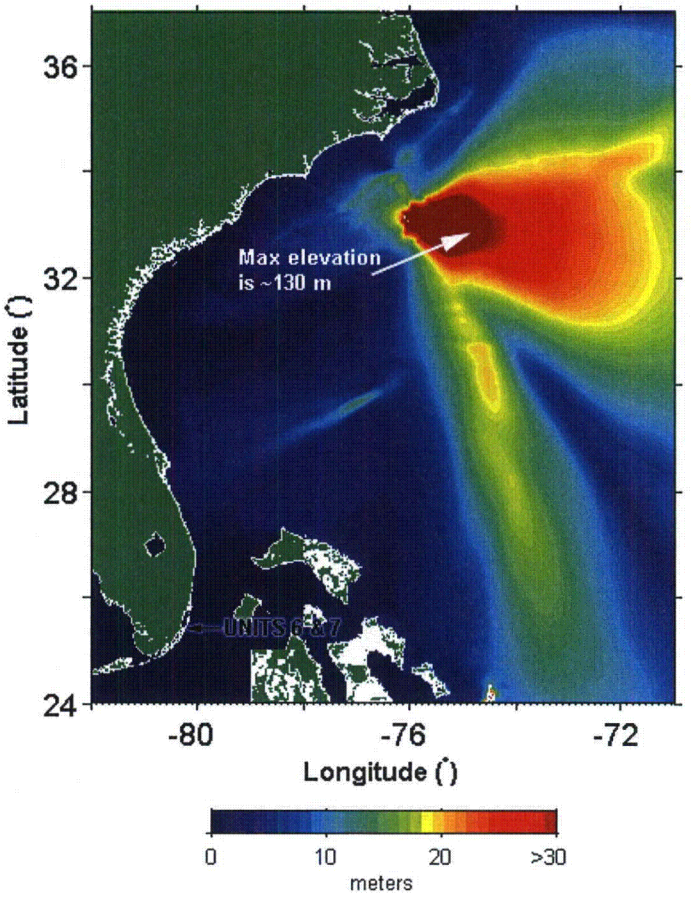

Figure 2.4.6-247. Simulated propagation of the Cape Fear tsunami (dynamic source) in Grid B at 100, 120, 140, 160, and 180 minutes after the submarine failure. Colors in elevation legend represent water surface elevations relative to MSL for ETOPO1 data and MLW for Coastal Relief Model data.

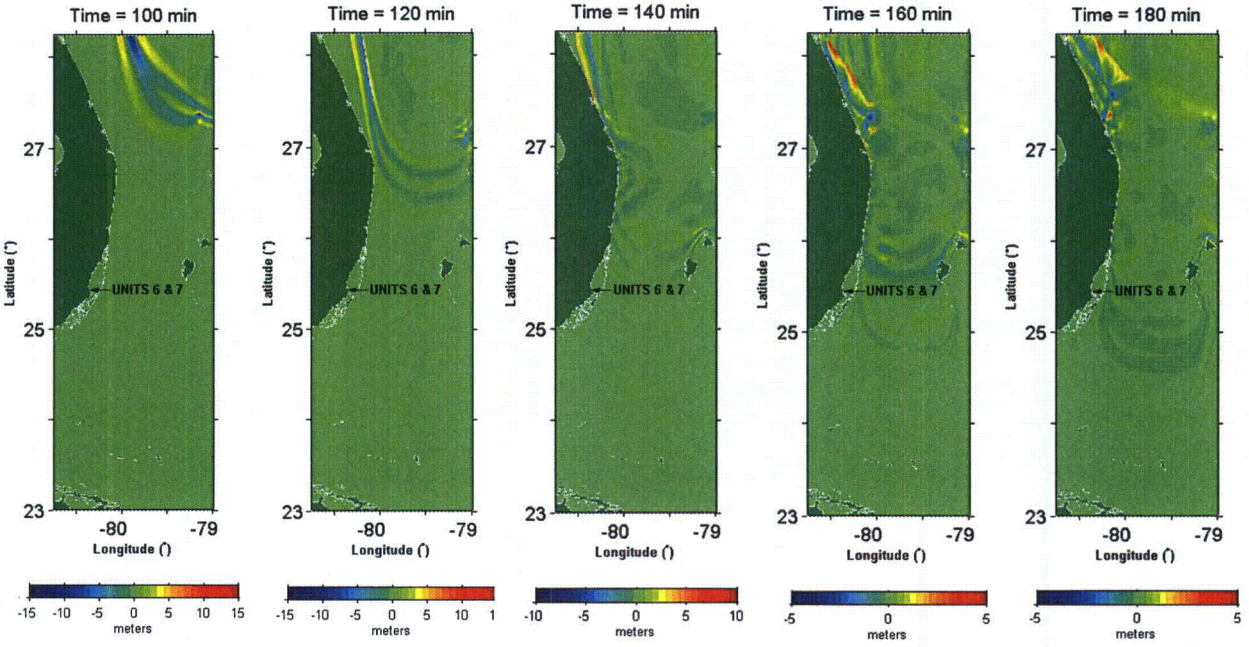

Figure 2.4.6-248. Simulated maximum water surface elevation during the propagation of the Cape Fear tsunami (dynamic source) in Grid B. Colors in elevation legend represent water surface elevations relative to MSL for ETOPO1 data and MLW for Coastal Relief Model data.

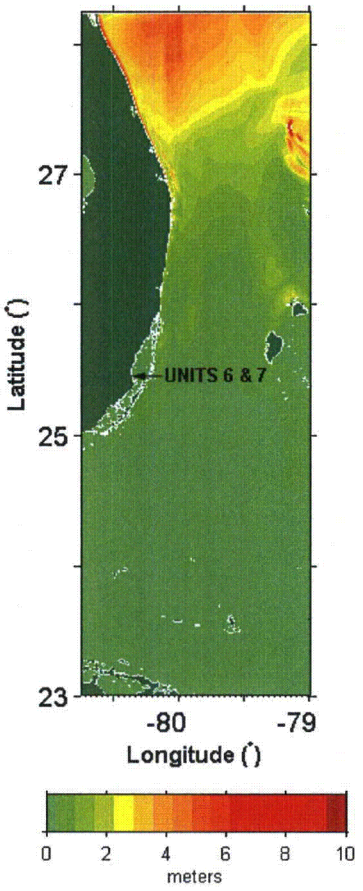

Figure 2.4.6-249. Simulated propagation of the Cape Fear tsunami (dynamic source) in Grid C at 140, 160, 180, 200, 220 and 240 minutes after the submarine failure. Colors in elevation legend represent water surface elevations relative to MLW.

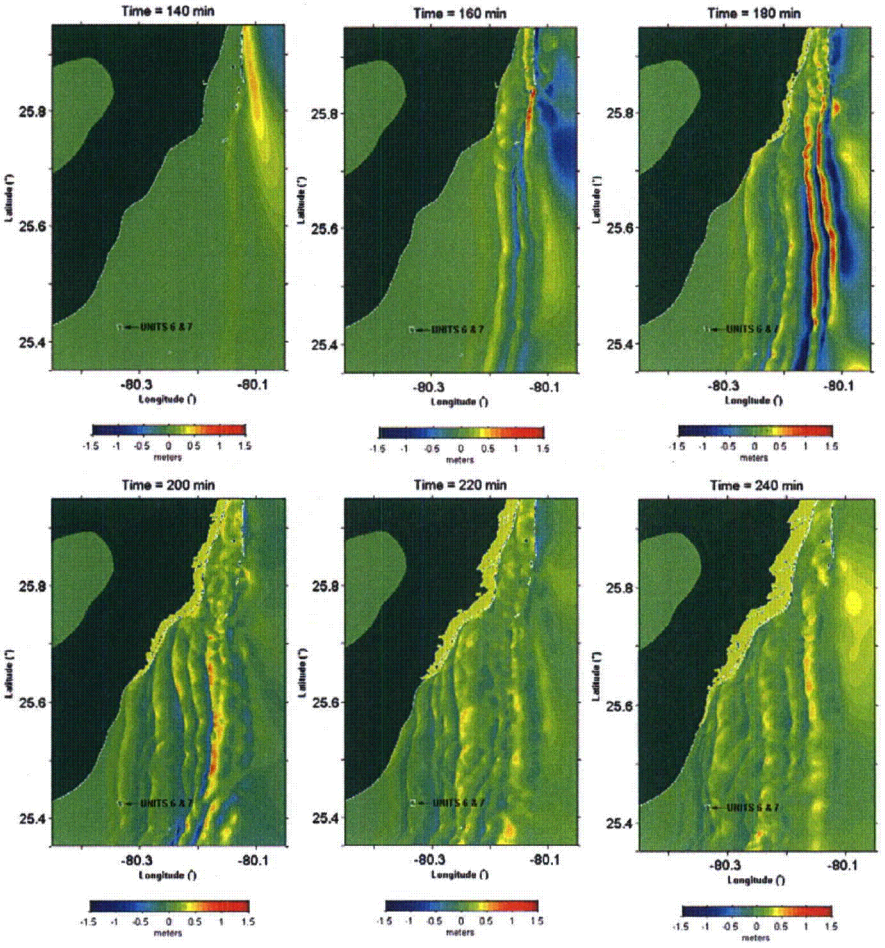

Figure 2.4.6-250. Simulated maximum water surface elevation during the propagation of the Cape Fear tsunami (dynamic source) in Grid C. Colors in elevation legend represent water surface elevations relative to MLW.

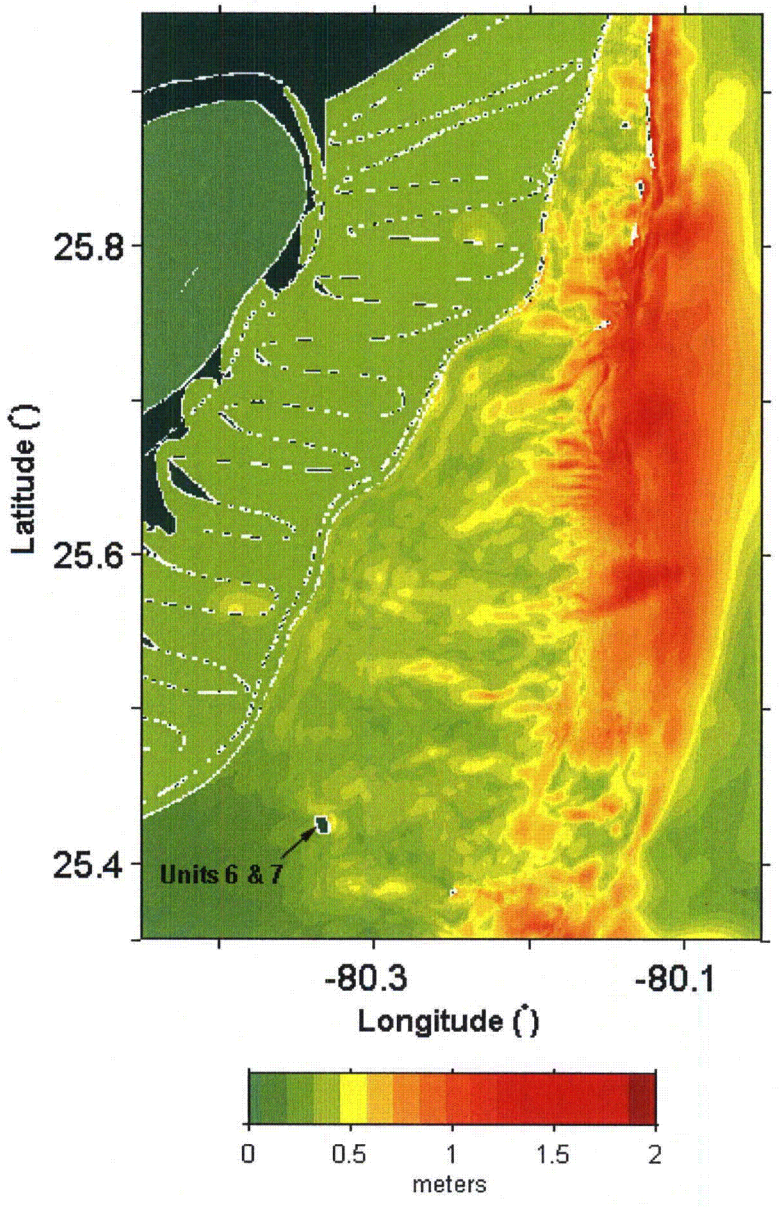

Figure 2.4.6-251. (a) Water depth relative to MLW over the area of Grid C; and (b) water depth relative to the assumed initial water surface in the Cape Fear tsunami simulations, i.e., 10 percent exceedance spring tide + sea rise + long-term sea level rise. Colors in elevation legend represent water surface elevations relative to MLW.

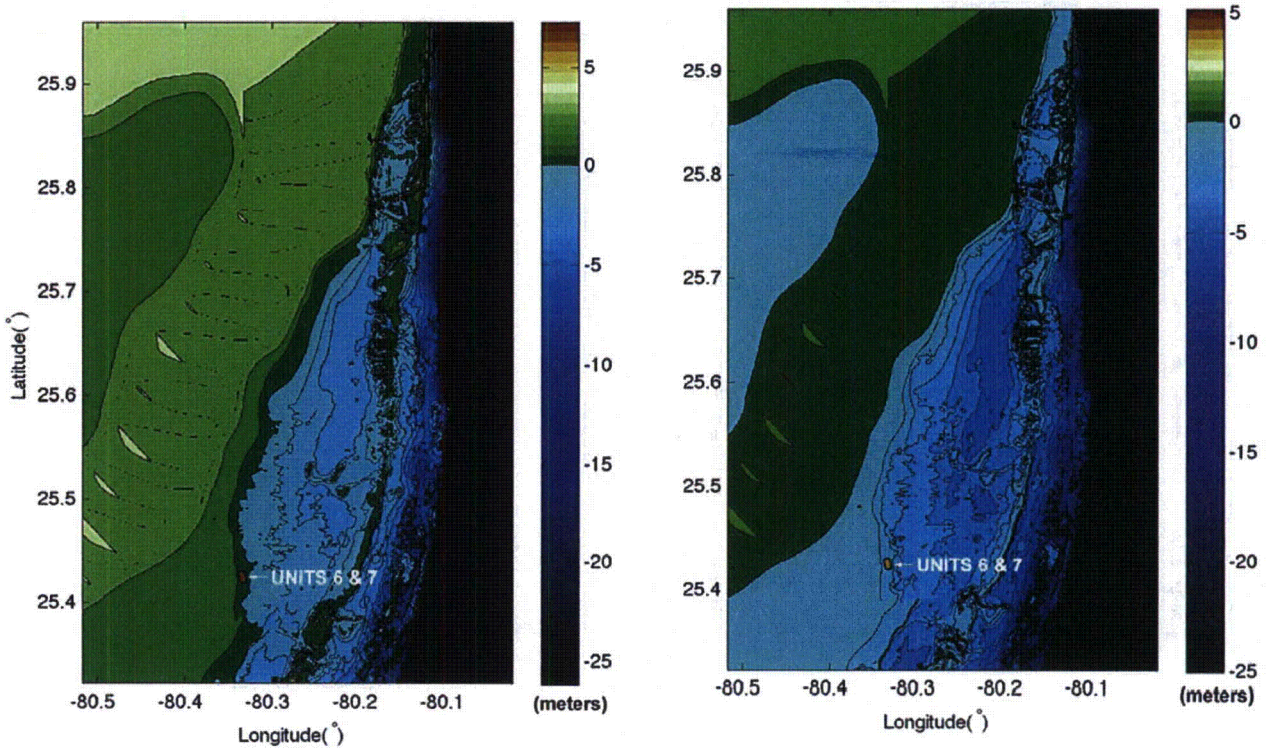

Figure 2.4.6-252. Simulated maximum water surface rise, relative to the initial sea water level, during the propagation of the Cape Fear tsunami (dynamic source) in the vicinity of Units 6 & 7. Colors in elevation legend represent water surface elevations relative to MLW.

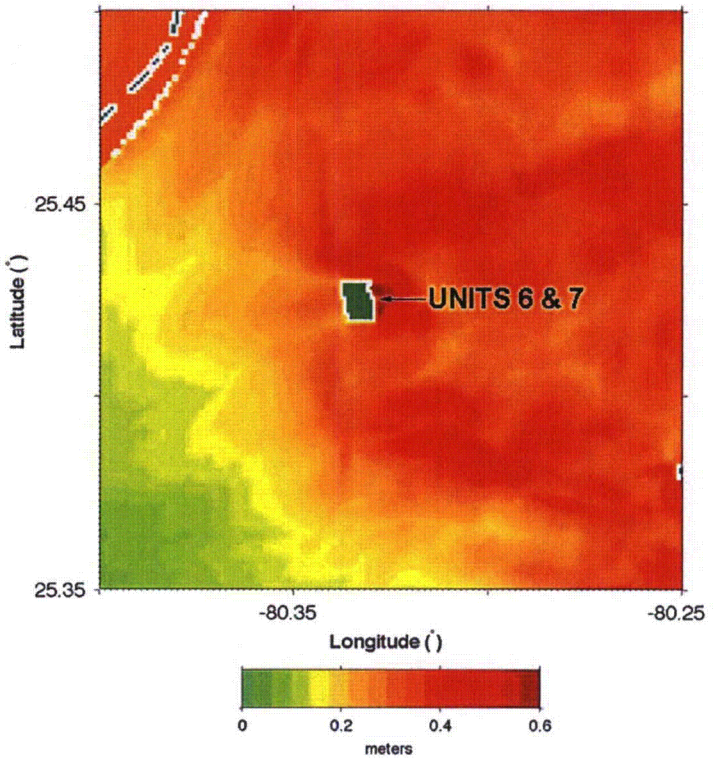

Figure 2.4.6-253. Water surface elevation near Units 6 & 7 as a function of time following the Cape Fear tsunami (dynamic source). Water surface elevations are relative to the initial water level.

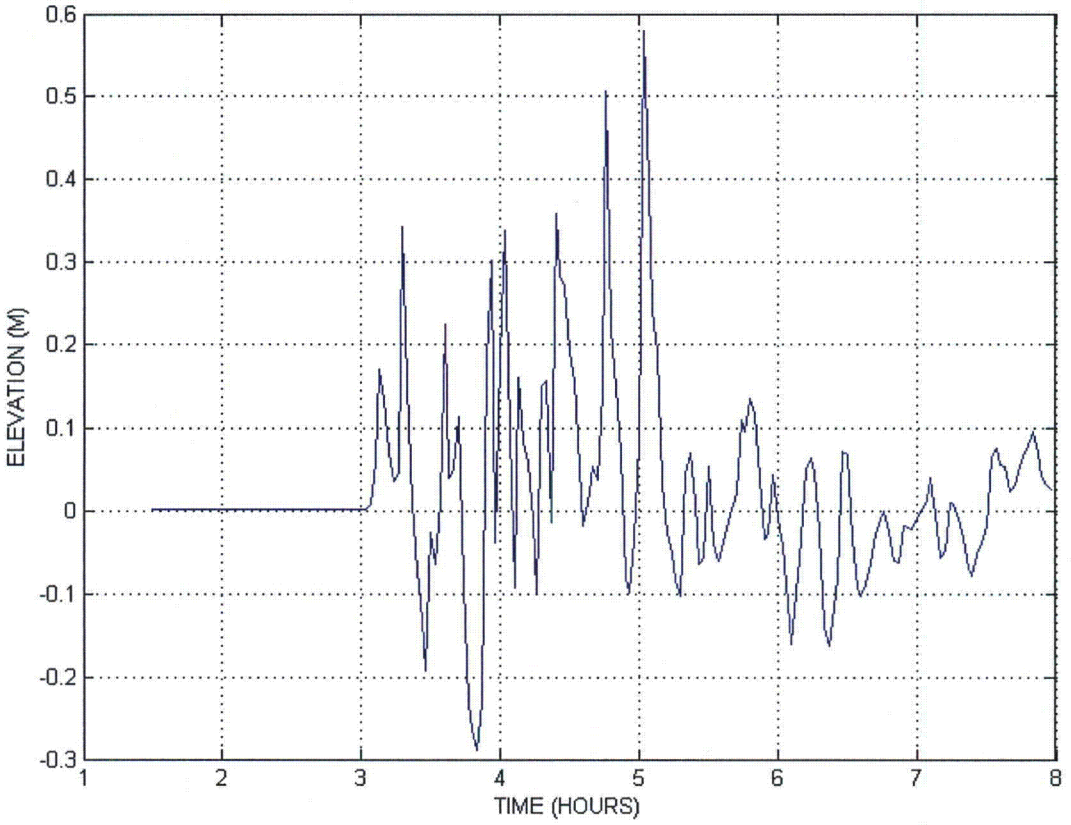

Figure 2.4.6-254. Simulated propagation of the Cape Fear tsunami (static source) in Grid A at 0, 20, 40, 60, 80 and 100 minutes after the submarine failure. Colors in elevation legend represent water surface elevations relative to MSL for ETOPO1 data and MLW for Coastal Relief Model data.

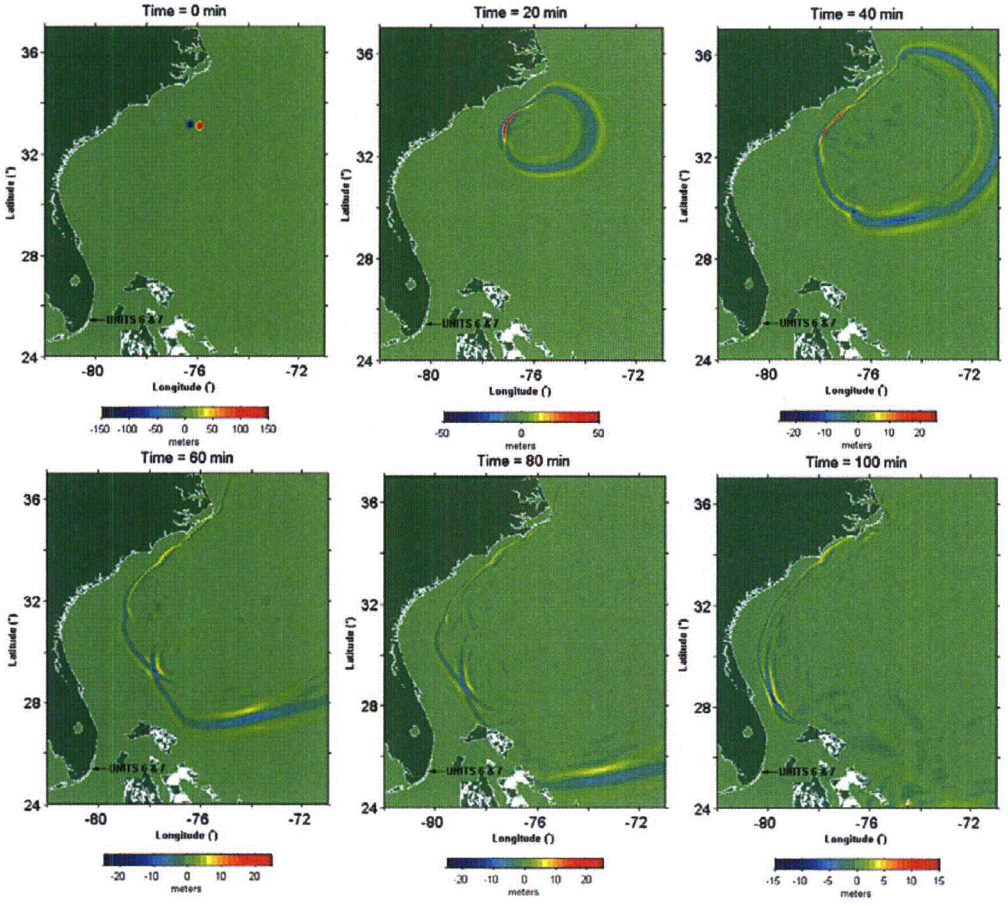

Figure 2.4.6-255. Simulated propagation of the Cape Fear tsunami (static source) in Grid A at 120, 140, 160, and 180 minutes after the submarine failure. Colors in elevation legend represent water surface elevations relative to MSL for ETOPO1 data and MLW for Coastal Relief Model data.

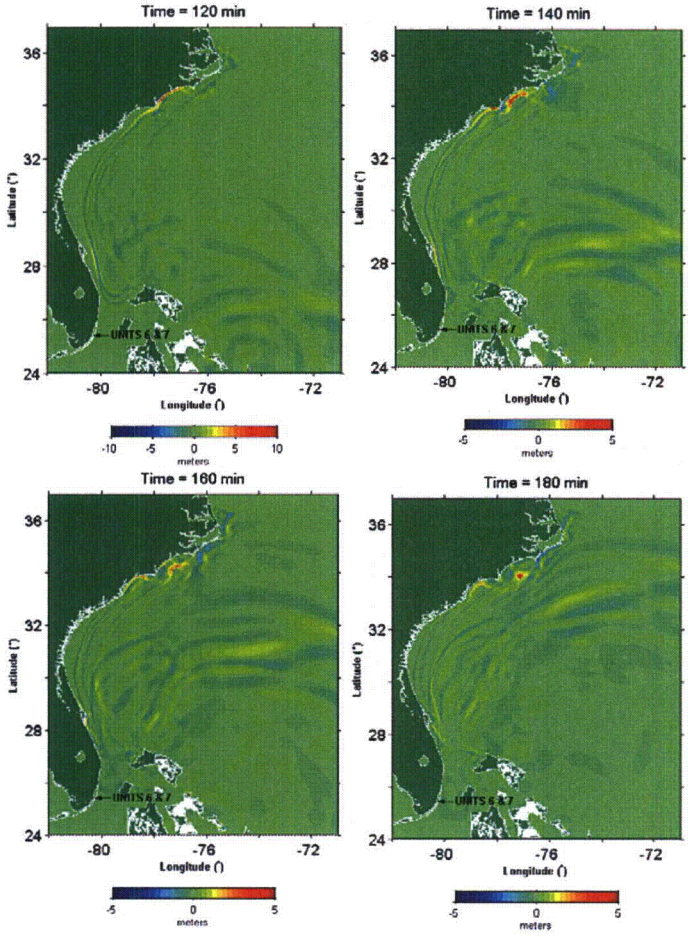

Figure 2.4.6-256. Simulated maximum water surface elevation during the propagation of the Cape Fear tsunami (static source) in Grid A. Colors in elevation legend represent water surface elevations relative to MSL for ETOPO1 data and MLW for Coastal Relief Model data.

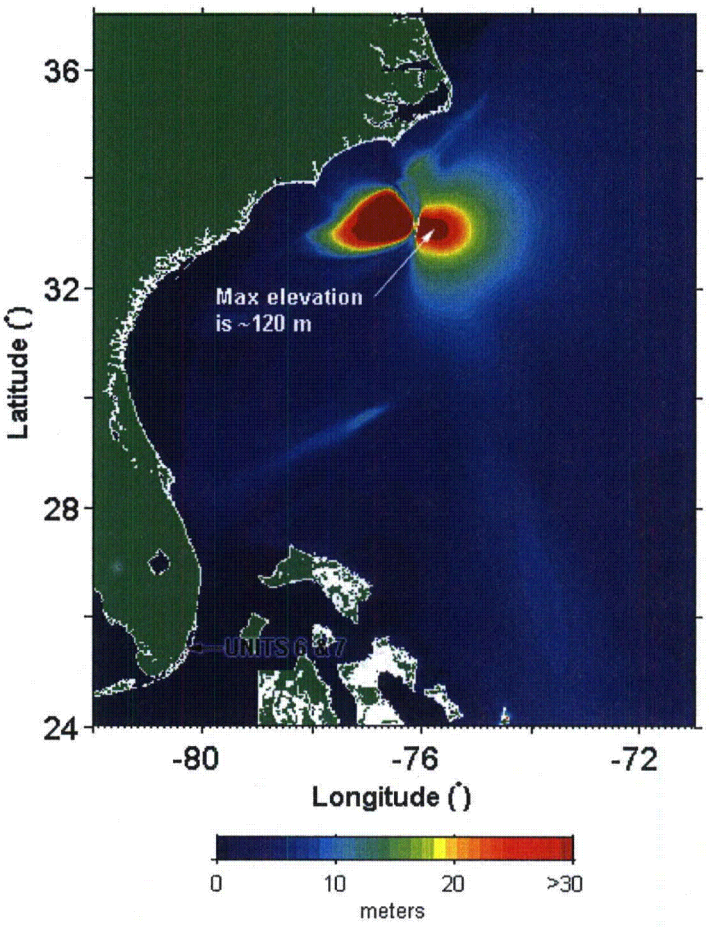

Figure 2.4.6-257. Simulated propagation of the Cape Fear tsunami (static source) in Grid B at 100, 120, 140, 160, and 180 minutes after the submarine failure. Colors in elevation legend represent water surface elevations relative to MSL for ETOPO1 data and MLW for Coastal Relief Model data.

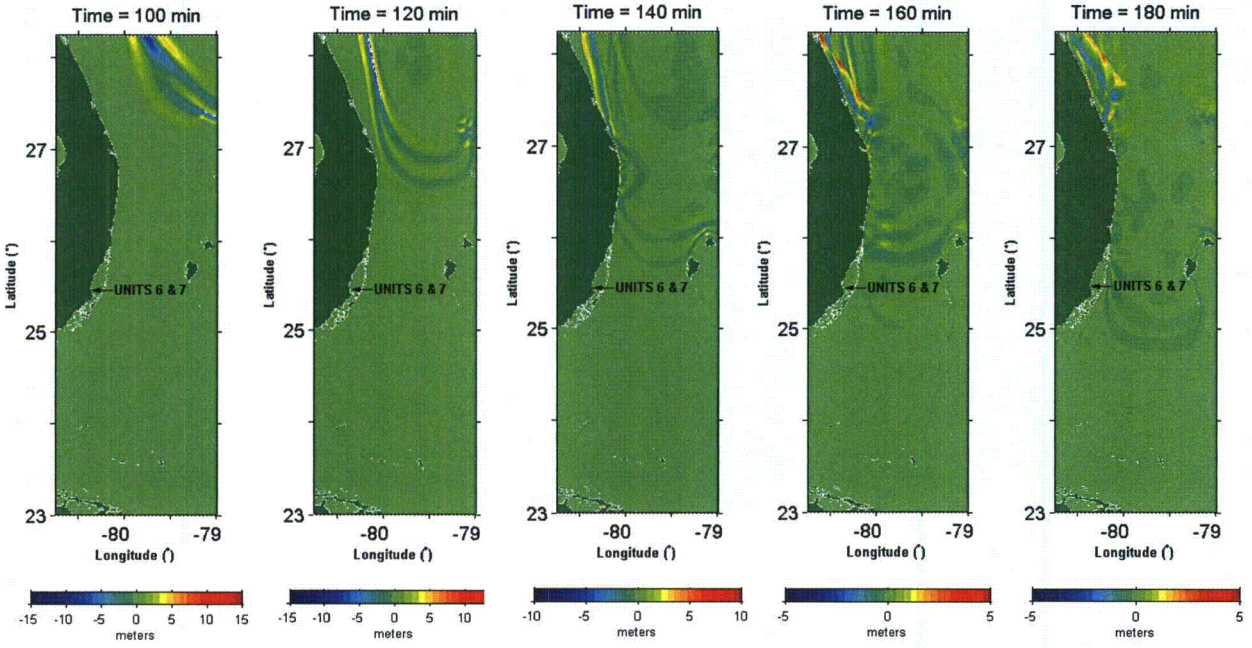

Figure 2.4.6-258. Simulated maximum water surface elevation during the propagation of the Cape Fear tsunami (static source) in Grid B. Colors in elevation legend represent water surface elevations relative to MSL for ETOPO1 data and MLW for Coastal Relief Model data.

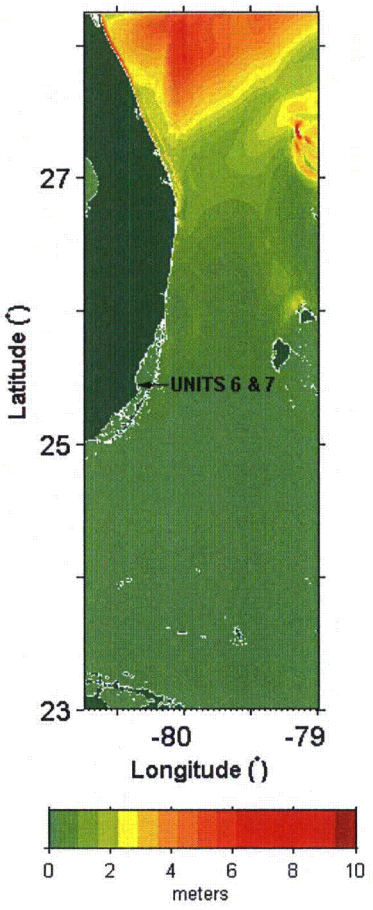

Figure 2.4.6-259. Simulated propagation of the Cape Fear tsunami (static source) in Grid C at 140, 160, 180, 200, 220 and 240 minutes after the submarine failure. Colors in elevation legend represent water surface elevations relative to MLW.

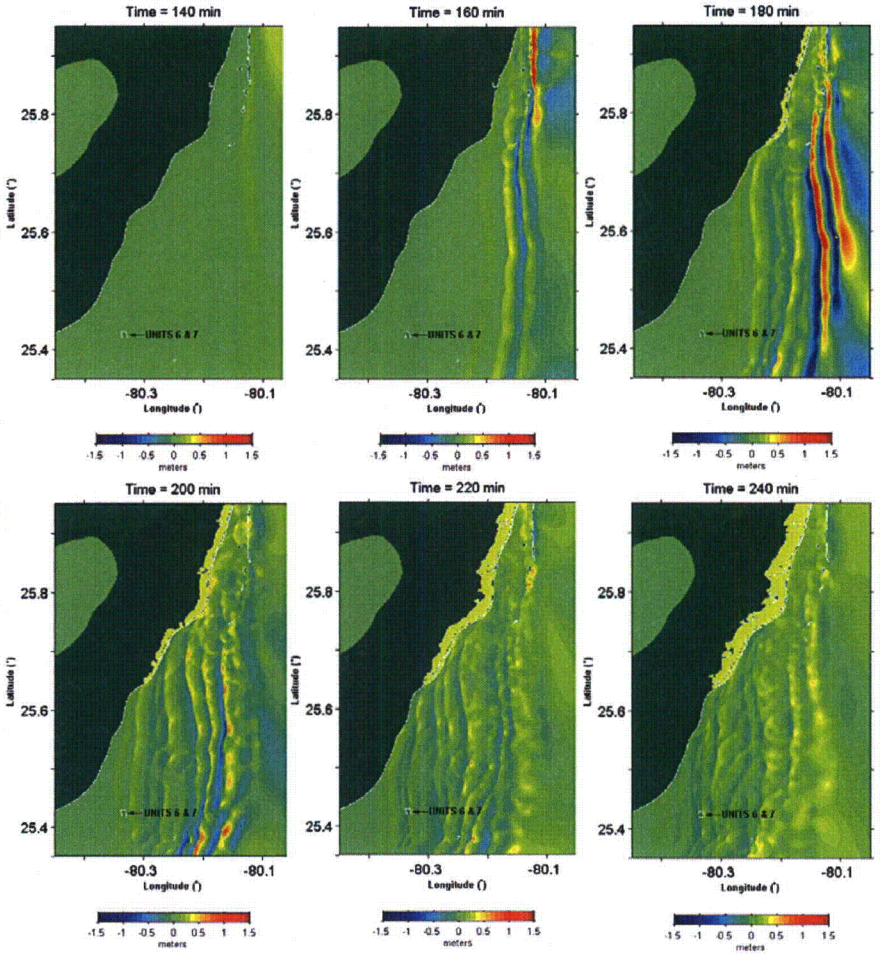

Figure 2.4.6-260. Simulated maximum water surface elevation during the propagation of the Cape Fear tsunami (static source) in Grid C. Colors in elevation legend represent water surface elevations relative to MLW.

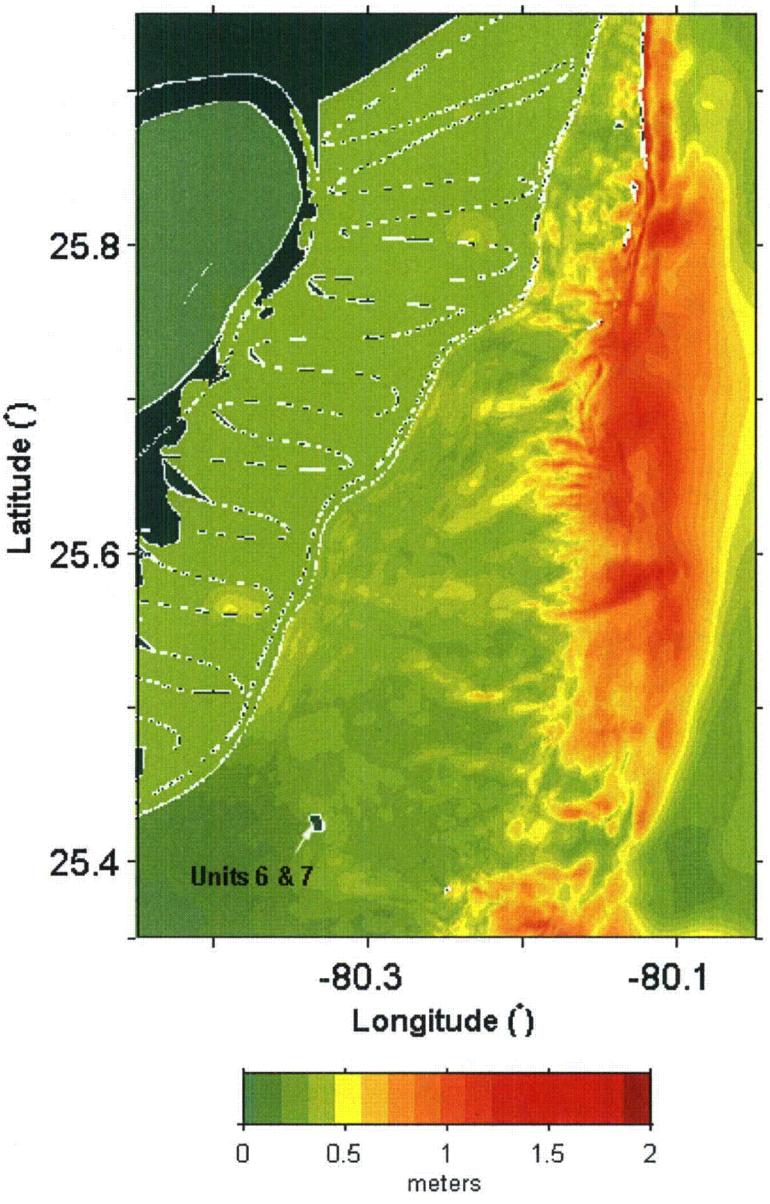

Figure 2.4.6-261. Simulated maximum water surface rise, relative to the initial sea water level, during the propagation of the Cape Fear tsunami (static source) in the vicinity of Units 6 & 7. Colors in elevation legend represent water surface elevations relative to MLW.

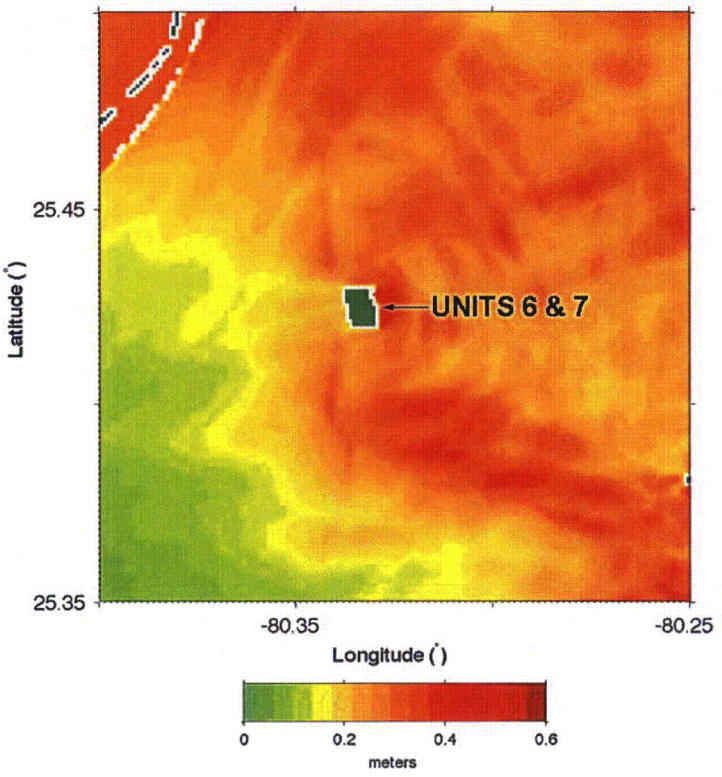

Figure 2.4.6-262. Water surface elevation near Units 6 & 7 as a function of time following the Cape Fear tsunami (static source). Water surface elevations are relative to the initial water level.

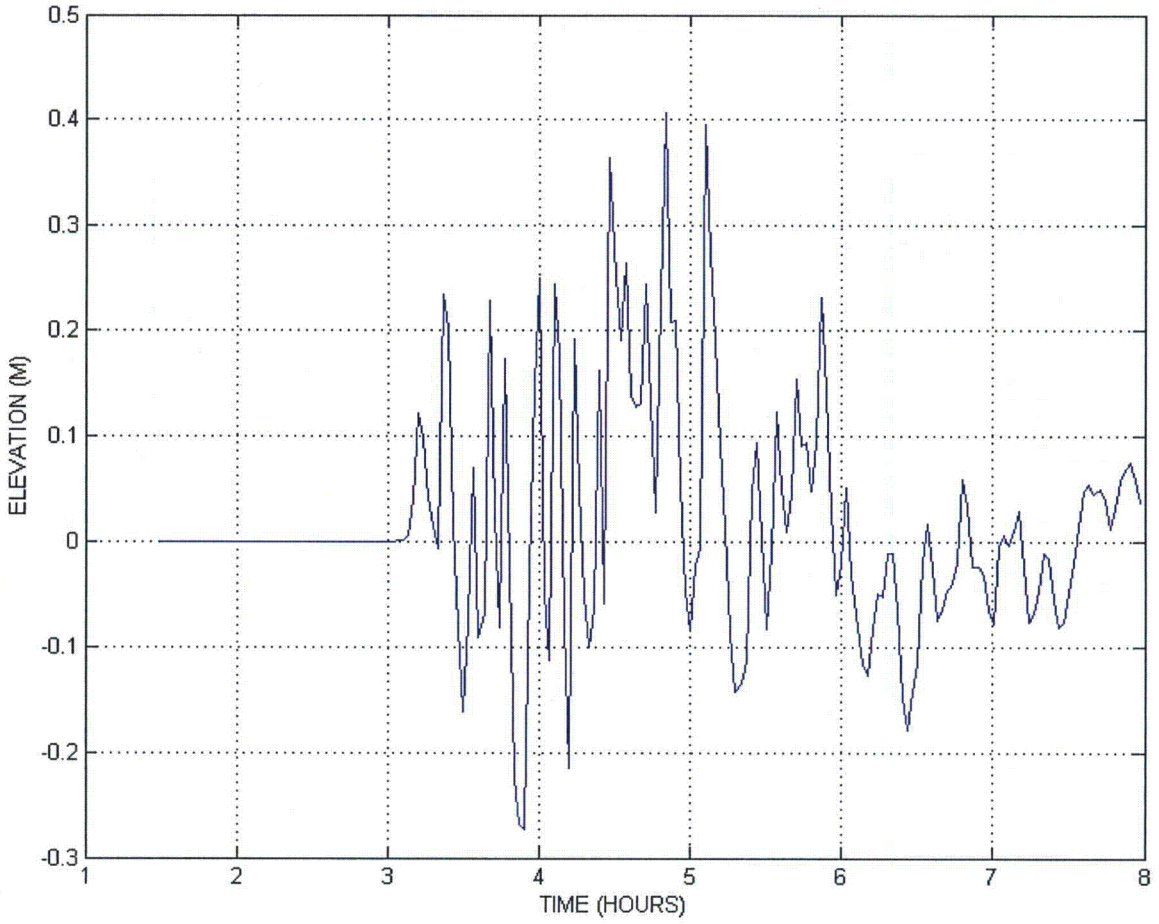

ASSOCIATED ENCLOSURES:

None